

Wind effect on tall buildings of square plan using computational fluid dynamics

by

Krishan Dutt Yadav
32EE22A01003

A Mini Project submitted to the
Academy of Scientific & Innovative Research
for the fulfillment of Minimum Credit
Required (4 credits) for IDDP
(M.Tech.+Ph.D.)
in
(ENGINEERING SCIENCE)

Under the supervision of
Dr. Bharat Singh Chauhan



Academy of Scientific and Innovative
Research AcSIR Headquarters, CSIR-HRDC
campus

Sector 19, Kamla Nehru Nagar,
Ghaziabad, U.P. – 201 002, India

2023-24

Certificate

This is to certify that the work incorporated in this Mini Project entitled, “Wind effect on tall buildings of square plan using computational fluid dynamics”, submitted by Krishan Dutt Yadav to the Academy of Scientific and Innovative Research (AcSIR) in fulfillment of the requirements for Minimum Credits (4 credits) of the Degree of Integrated Dual-Degree Program (M.Tech.+Ph.D.), embodies original research work carried-out by the student. We, further certify that this work has not been submitted to any other University or Institution in part or full for the award of any degree or diploma. Research material(s) obtained from other source(s) and used in this research work has/have been duly acknowledged in the Mini Project. Image(s), illustration(s), figure(s), table(s) etc., used in the thesis from other source(s), have also been duly cited and acknowledged.

(Signature of Student)

Krishan Dutt Yadav

(Signature of Supervisor)

Dr. Bharat Singh Chauhan

Dr. Nawal Kishor Banjara

(DAC Member)

Dr. Govind Gaurav

(DAC Member)

Dr. Suman Kumar

(DAC Member)

Dr. S. K. Panigrahi

(Laboratory Coordinator)

STATEMENTS OF ACADEMIC INTEGRITY

I Krishan Dutt Yadav, a IDDP (M.Tech.+Ph.D.) student of the Academy of Scientific and Innovative Research (AcSIR) with Registration No. 32EE22A01003 hereby undertake that, the Mini Project entitled “Wind effect on tall buildings of square plan using computational fluid dynamics” has been prepared by me and that the document reports original work carried out by me and is free of any plagiarism in compliance with the UGC Regulations on “*Promotion of Academic Integrity and Prevention of Plagiarism in Higher Educational Institutions (2018)*” and the CSIR Guidelines for “*Ethics in Research and in Governance (2020)*”.

Signature of the Student

Date :

Place :

It is hereby certified that the work done by the student, under my/our supervision, is plagiarism-free in accordance with the UGC Regulations on “*Promotion of Academic Integrity and Prevention of Plagiarism in Higher Educational Institutions (2018)*” and the CSIR Guidelines for “*Ethics in Research and in Governance (2020)*”.

Signature of the Supervisor

Name :

Date :

Place :

DECLARATION

I, Krishan Dutt Yadav, bearing AcSIR Registration No. 32EE22A01003
declare:

- (a) that the plagiarism detection software is currently not available at my work-place institute.
- (b) that my Mini Project entitled, “Wind effect on tall buildings of square plan using computational fluid dynamics” is plagiarism free in accordance with the UGC Regulations on “*Promotion of Academic Integrity and Prevention of Plagiarism in Higher Educational Institutions (2018)*” and the CSIR Guidelines for “*Ethics in Research and in Governance (2020)*”.
- (c) that I would be solely held responsible if any plagiarised content in my thesis is detected, which is violative of the UGC regulations 2018.

(Signature of the Student)

Date :

Place :

ACKNOWLEDGEMENTS

I would like to sincerely thank **Dr. M. K. DHAR**, Director of AcSIR university, and **Dr. S. K. PANIGRAHI**, Chief Scientist and AcSIR Coordinator of Central Building Research Institute, Roorkee, for their invaluable assistance in finishing my mini project, Wind effect on tall buildings of different aspect ratio using computational fluid dynamics.

My sincere gratitude goes out to my mentor, **Dr. Bharat Singh Chauhan**, for all of his time and hard work over the year. I greatly benefited from your insightful counsel and recommendations as I finished the Mini Project. In this aspect, I am eternally grateful to you.

I want to express my thanks to my Institute(Lab) Central Building Research Institute, Roorkee, for giving me opportunity to work.

I am grateful to Council of Scientific & Industrial Research (CSIR), India for monthly stipend money that help me financially.

Finally, but just as importantly, I want to thank my family, siblings, and friends for their tremendous help, and I sincerely appreciate everyone who helped to make this mini project a success.

(Signature of Student)

Krishan Dutt Yadav

ABSTRACT

Name of the Student: Krishan Dutt Yadav
Faculty of Study: Engineering Science
AcSIR academic centre/CSIR Lab: CBRI,
Roorkee

Registration No. : 32EE22A01003
Year of Submission: 2023
Name of the Supervisor(s): Dr. Bharat Singh
Chauhan

Title of the Mini Project: Wind effect on tall buildings of square plan using computational fluid dynamics

The current era of intense urbanisation is causing a rise in the need for structures in cities, which when combined with a shortage of available land for development, is causing the construction of tall and thin buildings. The wind loads are the main factor that influence the design of these tall buildings. Due to the high cost and time involved in experimentation and the simultaneous development of high computational capabilities, numerical simulations of wind flow around buildings have become more feasible and accurate. When compared to experimentation, the numerical solution provides a faster solution and results in substantially cheaper costs for large number of simulations. For numerical analysis, the current research project makes use of the commercially available ANSYS software and the open source CFD platform OpenFOAM. This project presents a research work that compares the two software platforms with the help of available literature for a square plan building. Both software platforms employ the RANS $k-\varepsilon$ turbulence model for simulation purpose. To obtain the results of the simulation, a uniform inlet velocity of 10 m/s is used. The post-processed results are displayed as streamlines and contour plots of wind pressure. By comparing with the Indian standard code it is found that the two software platforms are quite successful in the predicting the wind pressure contour plots and mean surface pressure coefficients (C_p) for various building faces. For each face of the building, the highest and lowest wind static pressure values are also determined. In certain features, the two platforms outperform one another as discussed in the Results and Discussion section. The near-façade pattern of airflow is accurately predicted in the current study with the help of stable RANS model. The vortex generation and wake recirculation within the domain were also predicted by the simulation results.

Keywords: CFD; OpenFOAM; ANSYS; RANS equation; $k-\varepsilon$ Turbulence Model.

LIST OF ABBREVIATIONS

Abbreviation	Description
CFD	Computational Fluid Dynamics
RMS	Root Mean Square
RANS	Reynolds Averaged Navier Stokes
LES	Large Eddy Simulation
DES	Detached Eddy Simulation
DNS	Direct Numerical Simulation
PLW	Pedestrian-level wind
LDA	Laser Doppler Anemometry
PIV	Particle Image Velocimetry
ANN	artificial neural networks
AOA	Angle of attack

LIST OF SYMBOLS

Symbol	Nomenclature	Units(MKS/CGS)
C_P	Pressure Coefficients	dimensionless
m	meter	meter
R_e	Reynolds Numbers	dimensionless
L	Length	meter
ρ	Density	Kg/m ³
U	Instantaneous Velocity	m/s
μ	Dynamic viscosity	Pascal-second(Pa-s)
k	Turbulence Kinetic Energy	J/kg or m ² /s ²
ε	Turbulence kinetic energy dissipation rate	m ² /s ³
u_i, u_j	Velocity Component	m/s
P	Air Pressure	Pa
t	Time	seconds
D_k	Diffusivity for k	dimensionless
$D\varepsilon$	Diffusivity for ε	dimensionless
C_1, C_2, C_μ and C_3	Model Coefficient	dimensionless
ν_t	Turbulent Viscosity	m ² /s

LIST OF FIGURES

Figure 1 Classification of flow based on Reynolds Number	2
Figure 2 Mean and Instantaneous Velocities	2
Figure 3 turbulence modelling in ANSYS	3
Figure 4 RANS based turbulence model in ANSYS Fluent.....	4
Figure 5 OpenFoam Case Directory	6
Figure 6 Prototype building with Wireframe Domain in ANSYS	11
Figure 7 Model of prototype building in ANSYS design modular with boundary conditions...	11
Figure 8 Prototype building with Computational Domain, Modelling in FreeCAD (Open Source)	12
Figure 9 Meshing of Prototype building with refinement in ANSYS Fluent.....	12
Figure 10 Tetrahedral Meshing with inflation (ANSYS)	13
Figure 11 Hexahedral Meshing with Inflation (ANSYS).....	13
Figure 12 Tetrahedral Meshing (Salome open source).....	14
Figure 13 SnappyHexMesh/HexaHedral Mesh(OpenFoam).....	14
Figure 14 Face description of the prototype building.....	15
Figure 15 Static pressure on Different Faces in Building at Bottom (0 m Height)	16
Figure 16 Coefficient of Pressure at different faces of prototype building	16
Figure 17 Static pressure Comparison of ANSYS Fluent and OpenFoam at different faces of prototype building at bottom (0 m height)	16
Figure 18 Cp Comparison of ANSYS Fluent and OpenFoam at bottom (0 m height)	17
Figure 19 Static pressure Comparison of ANSYS Fluent and OpenFoam at different faces of prototype building at mid height (5 m height)	17
Figure 20 Cp Comparison of ANSYS Fluent and OpenFoam at mid height (5 m height).....	17
Figure 21 Static pressure magnitude at vertical line at 5m distance/ Centre-line	18
Figure 22 Wireframe diagram of square plan building with XZ plane just at the surface of D face	18
Figure 23 Velocity streamline at surface of D Face	19
Figure 24 Pressure Contour of prototype building	19
Figure 25 Wireframe diagram of prototype building in paraview	20
Figure 26 Plane at Face D in paraview	20
Figure 27 streamline tracer (paraview).....	20
Figure 28 Drag Force calculation diagram showing steps involve in paraview	21
Figure 29 Drag Force calculation diagram showing steps involve in ANSYS Fluent	21
Figure 30 Value of Cp for different Faces as per Clause 7.3.3.1	26
Figure 31 Value of Drag Coefficient for building as per clause 7.4.2.....	26

LIST OF TABLES

Table 1 Basic theory of OpenFoam and ANSYS Fluent	6
Table 2 Cp at FACE A in OpenFoam.....	22
Table 3 Cp at Face A ANSYS	23
Table 4 Cp at Face B in OpenFoam.....	24
Table 5 Cp at Face C/D in OpenFoam.....	24
Table 6 Cp at FACE C/D ANSYS.....	25
Table 7 Cp at FACE B in ANSYS.....	25
Table 8 Value of Cp in different faces.....	26

CONTENTS

1. Chapter-1 Introduction
2. Chapter-2 Literature Review
3. Chapter-3 Methodology
4. Chapter-4 Results and Discussion
5. Chapter-5 Conclusion
6. Chapter-6 Reference

CHAPTER 1

INTRODUCTION

1.0 Introduction

The use of CFD (computational fluid dynamics), as an alternate for wind tunnel testing in many wind applications has been made possible by the significant advancement in the computing resources in the recent years. However, the domain size, the meshing technique, and the boundary conditions — the three primary components of a CFD simulation—are the fundamental factors that determine the accuracy of simulation ^[1]. This project discusses the fundamental theoretical underpinnings of using CFD simulations with constant input velocity and suggests the techniques for adopting building domains and meshing for CFD models in ANSYS and OpenFOAM. When the wind pressure distribution, streamlines, and wind velocity for a square plan tall building measuring 10m ×10m in plan and 10m in height is compared with the literature that is currently available, it is observed that OpenFOAM, an open-source CFD platform, performs as efficiently as ANSYS. This study illustrates the use of CFD simulation for flow visualisation around tall buildings. The quick development of computer technology makes it possible to solve rigorous mathematical equations involving complex flow conditions. However, most users view this useful tool as a black box due to their ignorance of the underlying theories and inherent features of CFD software. Later, this work will be extended for adopting the empirical relationship for atmospheric boundary layer, understanding the effect of different turbulence models and aspect ratio of the buildings.

1.1 A brief background of set-up in ANSYS and OpenFOAM

Since the project involves exploration of $k-\varepsilon$ turbulence model that is adopted on the two software platforms (1). ANSYS commercial software and (2). OpenFOAM open-source free software. The findings of both the software is compared and are validated with the available literatures. The two software platforms are found to perform equally well. Post-processing findings are presented in the Result and Discussion section of the project report.

1.1.1 Brief Introduction of ANSYS Fluent $k-\varepsilon$ turbulence model

ANSYS has two primary fluid flow solvers namely ANSYS Fluent and ANSYS CFX. In this study ANSYS Fluent is used as a CFD tool. Brief introduction of the adopted turbulence model is given in 1.1.1.1.

1.1.1.1 Identification of Turbulent Flow

External and internal flows along and around an obstacle are classified in *Fig. 1*.

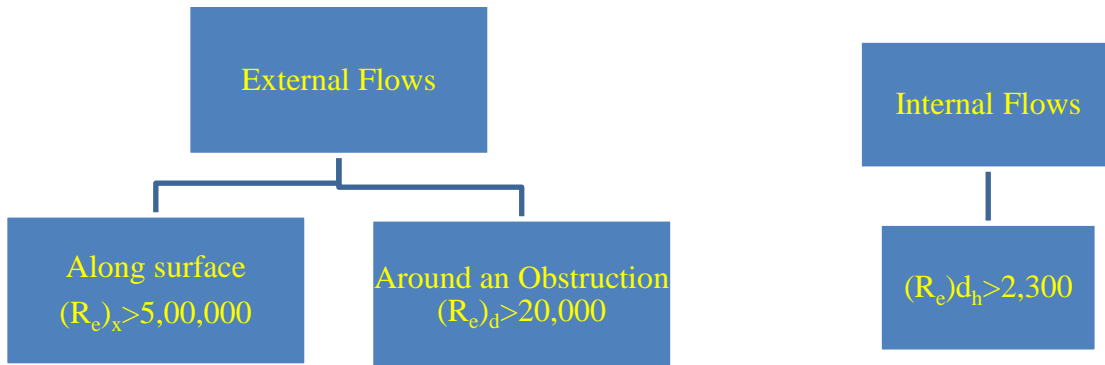


Figure 1 Classification of flow based on Reynolds Number

Where Reynolds Numbers $(Re)_L = \frac{\rho UL}{\mu}$

$L = x, d, d_h$, etc.

1.1.1.2 Instantaneous and Mean Velocities

- The instantaneous velocity (U), the measured velocity in the real (turbulent) fluid flow at a specific place (typical), would resemble this in *Fig.2*

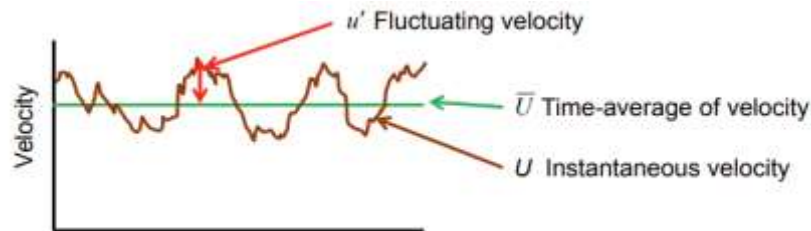


Figure 2 Mean and Instantaneous Velocities [2]

- At any instantaneous time: $U = \bar{U} + u'$
- The fluctuating velocity time average needs to be zero ($\overline{u'} = 0$)
- $\bar{u'}$'s RMS is not necessarily zero ($\overline{u'^2} \neq 0$)
- In a turbulent flow, the kinetic energy per unit mass of the turbulent fluctuations, u_i' is known as the turbulence kinetic energy, k . It is given by

$$k = \frac{1}{2} \overline{u'_i u'_i} = \frac{1}{2} [\overline{u'^2_x} + \overline{u'^2_y} + \overline{u'^2_z}] = \frac{3}{2} [\overline{u'^2}]$$

1.1.1.3 Approaches to turbulence modelling in ANSYS

All the turbulence modelling present in ANSYS is expressed in *Fig. 3*.

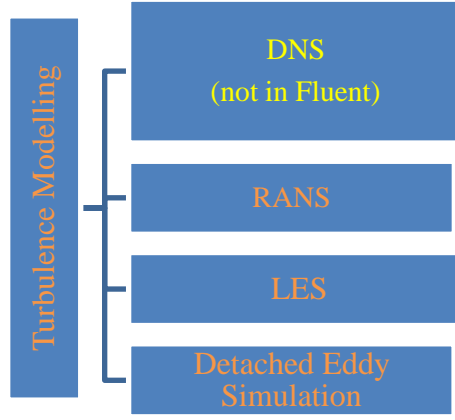


Figure 3 turbulence modelling in ANSYS [2]

Since this project involves RANS Turbulence modelling in ANSYS Fluent. So, the mathematics behind RANS ANSYS Fluent Modelling is discussed here.

The two primary governing equations of fluid dynamics are related to mass conservation (Eq. 1) and momentum (Eq. 2). The 2nd Eq. is also referred to as the fluid's Navier-Stokes Eq.

$$\frac{\partial \rho}{\partial t} + \frac{\partial(\rho u_i)}{\partial x_i} = 0 \quad \text{-----} (Eq. 1)$$

$$\frac{\partial(\rho u_i)}{\partial t} + \frac{\partial(\rho u_i u_j)}{\partial x_j} = -\frac{\partial P}{\partial x_i} + \frac{\partial}{\partial x_j} \left[\mu \left(\frac{\partial u_i}{\partial x_j} + \frac{\partial u_j}{\partial x_i} \right) \right] \quad \text{-----} (Eq. 2)$$

Time averaging

$$\bar{f} = \lim_{T \rightarrow \infty} \frac{1}{T} \int_0^T f(x_i, t) dt \quad \text{-----} (Eq. 3)$$

Instantaneous field of pressure and velocity as sum of mean and fluctuating component

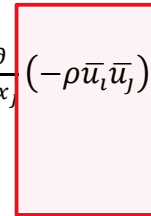
$$p = \bar{p} + p'$$

$$u_i = \bar{u}_i + u_i'$$

By averaging the mass conservation and Navier-Stokes equations (Eq. 1 and 2), averaged mass conservation equation and Averaged Navier-Stokes equation is obtained (Eq. 4 and 5).

$$\frac{\partial \rho}{\partial t} + \frac{\partial(\rho \bar{u}_i)}{\partial x_i} = 0 \quad \text{-----} (Eq. 4)$$

$$\frac{\partial(\rho \bar{u}_i)}{\partial t} + \frac{\partial(\rho \bar{u}_i \bar{u}_j)}{\partial x_j} = -\frac{\partial P}{\partial x_i} + \frac{\partial}{\partial x_j} \left[\mu \left(\frac{\partial \bar{u}_i}{\partial x_j} + \frac{\partial \bar{u}_j}{\partial x_i} - \frac{2}{3} \delta_{ij} \frac{\partial \bar{u}_m}{\partial x_m} \right) \right] + \frac{\partial}{\partial x_j} \left(-\rho \bar{u}_i' \bar{u}_j' \right) \quad \text{-----} (Eq. 5)$$



Reynolds
stress tensor, R_{ij}

RANS based models present in ANSYS Fluent

Different RANS based turbulence model present in ANSYS Fluent specially presented in Fig.

4.

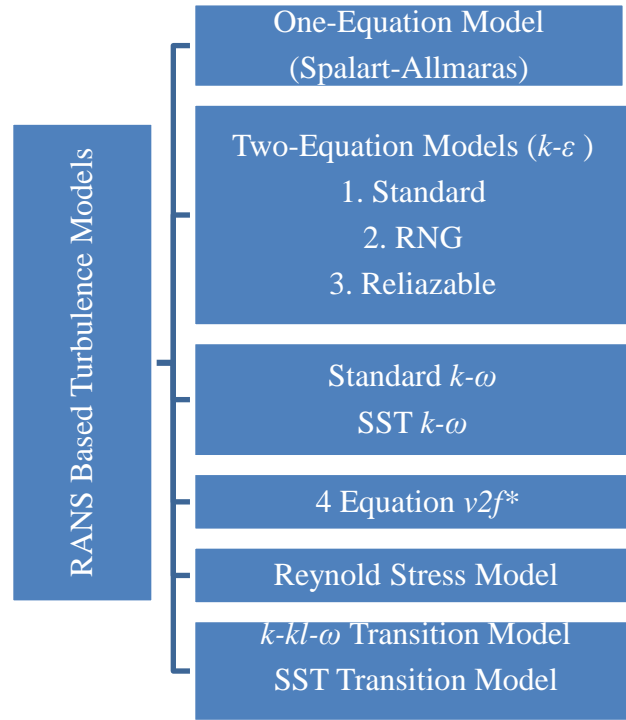


Figure 4 RANS based turbulence model in ANSYS Fluent

1.1.2 Brief Introduction of OpenFOAM k - ε turbulence model

The free, open-source CFD program OpenFOAM was mainly created by OpenCFD Ltd. It is having all turbulence model as ANSYS except DNS Model [3].

1.1.2 k - ε turbulence model transport equations in OpenFOAM and ANSYS

All the basic mathematical partial differential equation used in ANSYS Fluent and OpenFoam is presented in table 1.

OpenFOAM [3]	ANSYS Fluent [2]
<p>Model equation for Turbulence kinetic energy, k</p> $\frac{D}{Dt}(\rho k) = \nabla \cdot (\rho D_k \nabla k) + P - \rho \varepsilon \quad \text{-----}$ <p>(Eq. 6)</p> <p>OpenFOAM implementation of Turbulence kinetic energy, k obtained from (Eq. 6 (i))</p> $\frac{\partial}{\partial t}(\alpha \rho k) + \nabla \cdot (\alpha \rho u k) - \nabla^2(\alpha \rho D_k k) =$ $\alpha \rho G - \left(\frac{2}{3} \alpha \rho \nabla \cdot u k\right) - \alpha \rho \frac{\varepsilon}{k} k + S_k + S_{fvOptions}$ <p>S_k= internal source term pertaining to k</p>	<p>Turbulence kinetic energy, k obtained from (Eq. 9) transport equation</p> $\frac{\partial(\rho k)}{\partial t} + \frac{\partial(\rho k u_i)}{\partial x_i} = \frac{\partial}{\partial x_j} \left[\left(\mu + \frac{\mu_t}{\sigma_k} \right) \left(\frac{\partial k}{\partial x_j} \right) \right] + G_k + G_b - \rho \varepsilon - Y_M + S_k \quad \text{-----}$ <p>(Eq. 9)</p>

<p>$S_{fvOptions}$=Source term introduced by $S_{fvOptions}$ for k</p>	
<p>Turbulence kinetic energy dissipation rate, ε obtained from (Eq. 7) transport equation</p> $\frac{D}{Dt}(\rho k) = \nabla \cdot (\rho D_\varepsilon \nabla \varepsilon) + \frac{c_1 \varepsilon}{k} \left(P + C_3 \frac{2}{3} k \nabla \cdot u \right) - C_2 \rho \frac{\varepsilon^2}{k} \text{-----}(Eq. 7)$ <p>OpenFOAM implementation of Turbulence kinetic energy dissipation rate, ε obtained from (Eq. 7(i))</p> $\frac{\partial}{\partial t}(\alpha \rho \varepsilon) + \nabla \cdot (\alpha \rho u \varepsilon) - \nabla^2(\alpha \rho D_\varepsilon \varepsilon) = C_1 \alpha \rho G \frac{\varepsilon}{k} - \left(\left(\frac{2}{3} C_1 - C_{3, RDT} \right) \alpha \rho \nabla \cdot u \varepsilon \right) - C_2 \alpha \rho \frac{\varepsilon}{k} \varepsilon + S_\varepsilon + S_{fvOptions}$ <p>α= The specified phase's phase fraction G=Anisotropic component of the Reynolds-stress tensor causes turbulent kinetic energy production at a turbulent rate (m^2/s^3).</p> <p>D_k is diffusivity for k D_ε is diffusivity for ε C_1, C_2, C_μ and $C_{3, RDT}$(Rapid-distortion theory compression term coefficient) are model coefficients</p> <p>$C_1=1.44, C_2=1.92, C_\mu=0.09, C_{3, RDT}=0, \sigma_k=1.0, \sigma_\varepsilon=1.3$</p> <p>$S_\varepsilon$=internal source term pertaining to ε $S_{fvOptions}$=Source term introduced by $S_{fvOptions}$ for ε</p>	<p>Turbulence kinetic energy dissipation rate, ε obtained from (Eq. 10) transport equation</p> $\frac{\partial(\rho \varepsilon)}{\partial t} + \frac{\partial(\rho \varepsilon u_i)}{\partial x_i} = \frac{\partial}{\partial x_j} \left[\left(\mu + \frac{\mu_t}{\sigma_\varepsilon} \right) \left(\frac{\partial \varepsilon}{\partial x_j} \right) \right] + c_{1\varepsilon} \frac{\varepsilon}{k} [G_k + c_{3\varepsilon} G_b] - c_{2\varepsilon} \rho \frac{\varepsilon^2}{k} + S_\varepsilon \text{-----}(Eq. 10)$ <p>The mean velocity gradients' produced turbulent kinetic energy is denoted by G_k.</p> <p>G_k calculated by</p> $G_k = -\rho \bar{u}_i \bar{u}_j \frac{\partial u_j}{\partial x_i}$ <p>The fluctuation dilatation in compressible turbulence's contribution to the total dissipation rate is denoted by Y_M.</p> $Y_M = 2\rho \varepsilon M_t^2$ <p>Where M_t is turbulent Mach Number calculated by $M_t = \sqrt{\frac{k}{a^2}}$</p> <p>$a$ is speed of sound ($a = \sqrt{\gamma RT}$)</p>
<p>Turbulent viscosity ν_t obtained from (Eq. 8)</p> $\nu_t = C_\mu \rho \frac{k^2}{\varepsilon} \text{-----}(Eq. 8)$	<p>Turbulent viscosity μ_t obtained from (Eq. 11)</p> $\mu_t = C_\mu \rho \frac{k^2}{\varepsilon}$

<p>initial condition for k, (for isotropic turbulence)</p> $k = \frac{3}{2} (I u_{ref})^2$ <p>Initial condition for ε, (for isotropic turbulence)</p> $\varepsilon = \frac{C_\mu^{0.75} k^{1.5}}{L}$ <p>I= Turbulence Intensity (%)</p> <p>u_{ref}= A reference flow speed (m/s)</p> <p>L= a reference length scale (m)</p>	<p>model constants have following default values</p> $C_{1\varepsilon}=1.44, C_{2\varepsilon}=1.92, C_\mu=0.09, \sigma_k=1.0,$ $\sigma_\varepsilon=1.3 \text{ and } c_{3\varepsilon} = \tanh \left \frac{v}{u} \right $ <p>For buoyant shear layers perpendicular to the gravitational vector $c_{3\varepsilon}$ will equal 0.</p> <p>S_k and S_ε are user defined source terms.</p>
--	--

Table 1 Basic theory of OpenFoam and ANSYS Fluent

Instead of being kept in a single case file, OpenFOAM data is kept as a collection of files inside a case directory. The necessary data can be found in the three directories shown in Fig. 5 under the appropriately descriptive name assigned to the case directory:

- constant
- system, and
- initial time directory, e.g.0.

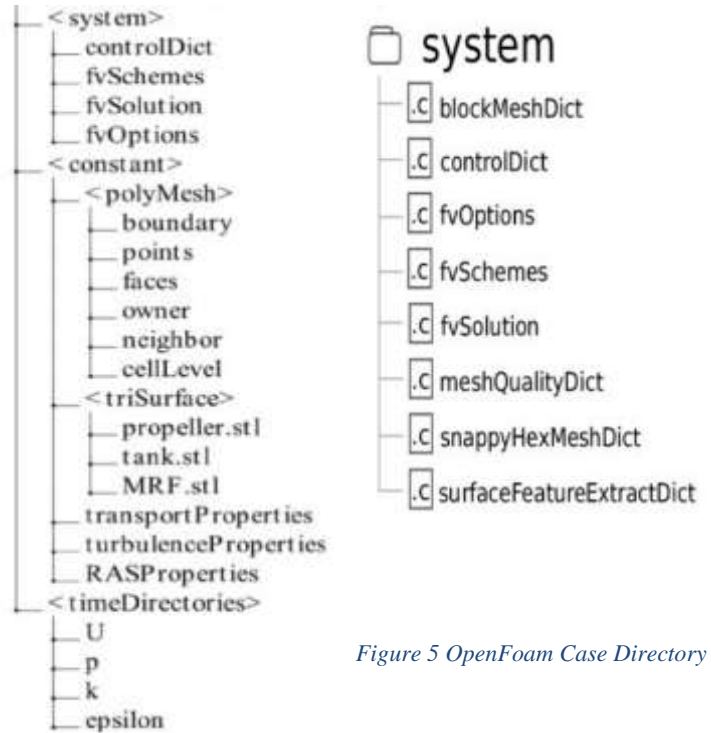


Figure 5 OpenFoam Case Directory

CHAPTER 2

LITERATURE REVIEW

Weerasuriya, A. U. (2013, July 30): The main topic of this work is the atmospheric boundary layer simulation using computational fluid dynamics (CFD). It discusses the recommended methods for creating domains and meshes for CFD models, as well as empirical techniques that can serve as boundary conditions in the lack of reliable data. The study finds that empirical approaches function satisfactorily when comparing the findings of wind tunnel tests with the pressure distribution simulations from CFD on 112m tall buildings. The research also demonstrates the application of CFD modeling to pedestrian level wind velocity evaluation and flow visualization around tall buildings ^[1].

Blocken, B.B. et al. (2016): The research paper discusses wind-tunnel and computational fluid dynamics (CFD) techniques used to determine pedestrian-level wind (PLW) speeds in the presence of buildings. It mentions that the accuracy of low-cost wind-tunnel techniques and steady RANS simulations can diminish at lower amplification factors (<1), but they still provide accurate results ($\sim 10\%$) at high amplification factors (>1). According to the article, this does not affect the precision of the PLW comfort assessment, as higher amplification factors have a greater impact on discomfort exceedance probability. While techniques such as LDA, PIV, and LES are more accurate, the paper advocates for the continued use of faster and less expensive techniques for PLW studies. In terms of turbulent flows, it concludes that pedestrian-level wind comfort is an area where nature is comparably kind to us ^[4].

Zaki, A. et al. (2023): The research presented in this article focuses on the ventilation flows in a structure that has building arrays surrounding a windcatcher. Two forms of surrounding building arrangements, inline and staggered, were studied to represent different suburban morphologies. There were five potential wind directions for which ventilation measurements were made: two normal, two oblique, and one parallel to the building opening(s). The analysis of the data was performed using both time-averaged and instantaneous approaches. While the instantaneous data analysis allowed for the exploration of unsteady airflow features, such as changes in room pressure, the time-averaged analysis demonstrated the overall interaction of ventilation flow with the building. According to the findings, the maximum ventilation rate reductions for inline and staggered arrays, respectively, were 30% and 42% when compared to an isolated building example ^[6].

Calzolari, G. et al. (2023): The main points of the research input highlight the critical review of deep learning approaches in fluid mechanics simulations and propose alternative techniques for built environment applications. The study reveals that artificial neural networks (ANNs) have the potential to enhance turbulence models for more accurate coupled computational fluid dynamics (CFD) simulations. Through physics-informed deep learning modeling, they can also increase the effectiveness of Proper Orthogonal Decomposition (POD) techniques and take advantage of significant physical attributes and data. Additionally, deep learning enables the exploration of advanced flow analysis methods such as super-resolution techniques. However, challenges exist, including the need for consistent large flow databases, the problem of extrapolation tasks, and the risk of over-fitting. This research suggests that further investigation is necessary to fully explore the potential of deep learning in the built environment field ^[5].

Yuan, Y. et al. (2022): This study focuses on developing a set of inflow boundary conditions based on RANS simulations with a focus on horizontal uniformity in particular, to resemble the twisted wind field. Additionally, the study aims to predict the aerodynamic forces acting on a squared tall building using these simulated twisted winds. These findings show that the horizontal homogeneity of the inflow conditions for twisting winds at the ground surface can be greatly enhanced by suitably modifying the turbulence dynamic viscosity in the Murakami-Mochida-Kondo (MMK) model. Furthermore, a precise simulation of the twisted wind-induced flow around the building and the related wind pressure distribution is made possible by the created boundary conditions in conjunction with the use of the MMK turbulence model. When it comes to forecasting the aerodynamic forces on the squared tall building under twisted winds, the expanded inflow boundary conditions applied to the SST $k-\omega$ model likewise show good agreement with experimental results ^[7].

Zaki, A. et al. (2023): Under atmospheric boundary layer flow, the study examines how horizontal ribs affect the flow field and wind force of tall buildings using the Large Eddy Simulation (LES) approach. The findings reveal that the presence of horizontal ribs significantly affects the flow patterns. The ribs enlarge the vortex in the near wake and prevent the separation vortex from forming near to the sidewall. Close to the building face, they obstruct the vertical flow and create a tiny recirculation around the ribs, creating a focus between adjacent ribs. As a result, the near-wall flow pattern undergoes a considerable alteration. Significant changes in wind force and wind pressure distribution result from this variance in near-wall flow. According to the study, the addition of horizontal ribs may result in a "Zigzag" pattern of mean pressure along the height of the structure and reduce the fluctuating lift by up to 27%. Continuous ribs have a more pronounced effect on reducing wind load compared to discontinuous ribs. Overall, this research demonstrates the influence of horizontal ribs on the near-wall flow, vortex structure, wind pressure distribution, and wind force of high-rise buildings ^[8].

Wijesooriya, K. et al. (2021): The primary focus of the research input pertains to the numerical validation of an efficient uncoupled fluid-structure interaction (FSI) method that is employed in assessing the structural reactions of extremely tall structures. A boundary layer wind tunnel is used to evaluate an aeroelastic multi-degree of freedom model and comparing its results with a numerical simulation. The study is innovative in that it shows how to effectively calculate structural responses by communicating wind pressures to the structural model. An innovative method is used to translate wind-induced pressures into nodal time history loads that execute an implicit modal analysis and extract the time history response of the structure. The newly suggested technique reportedly achieves accurate results quickly compared to traditional experiments. Additionally, the paper examines vortex-induced vibrations, aerodynamic damping, and structural damping impacts on the structure's performance, ultimately demonstrating that this numerical method could serve as an efficient alternative to full aeroelastic wind tunnel studies for assessing super-tall structures' structural responses ^[9].

Chauhan, B.S. et al. (2020): The investigation of interference's impact on various tall building components with a rectangular cross-sectional shape is the paper's main area. The study investigates how wind loads are changed and how the major structure's components react when an interfering building is present in close proximity to principal building components. The two building models are arranged in an L-shape in plan to simulate real-life scenarios. By varying the height of the interfering buildings with respect to the principal building, the researchers were able to study and analyse the response of different components of the principal building. The findings, which are displayed as *X-Y* plots, demonstrate the significantly increased reaction of the main building elements with regard to the across-wind force's effects on bending moment, twisting moment, and across-wind displacement ^[10].

Chauhan, B.S. et al. (2023): The research focuses on understanding the wind interference phenomenon in rectangular tall buildings commonly used by engineers and architects. In order to conduct the study, interfering buildings with the same height and cross-section form as the principal building are tested in wind tunnels. Initially forming a *U* shape, these interfering buildings are placed in front of the principal building. The experiment varies the position of the interfering buildings in two ways: by moving both buildings simultaneously towards each other and by keeping one building stationary while varying the position of the other. Two types of measurements, force measurement and pressure measurement, are conducted independently. The experimental results are compared to validate the findings. According to the force measurement, the principal building's across wind force may increase by up to 2.18 times compared to the isolated condition, and the twisting moment also significantly increases, up to 39.43 times. Contour plots for the coefficient of mean wind pressure provide a clear understanding of the results obtained through force measurement ^[11].

Chauhan, B.S. et al. (2023): The research paper investigates the change in wind loads on a tall building as a result of two nearby interfering buildings differing heights. The study is conducted using three building models placed in a *U* shape plan. There are two ways to vary the heights of the building models that interfere: either simultaneously reducing both of their heights or reducing the height of only one interfering building model. Wind tunnel experiments are conducted, and the results are presented in the form of *X-Y* plots. The findings reveal that as the height difference between the interfering buildings increases, there is an increase in the torsional moment caused by the interference effect. Additionally, because of the shielding effect, the height of the interfering structures reduces the along wind force^[12].

Mukherjee, S. et al. (2014): The primary focus of the research input is a thorough examination of the pressure exerted on the various faces of a tall building with a '*Y*' plan shape. The Indian Institute of Technology Roorkee's boundary layer wind tunnel is the site of an experiment that is part of the study, which combines numerical and experimental methods. With a mean wind velocity of 10 m/s, the flow condition is consistent with terrain type II of IS:875 (Part 3) - 1987. Furthermore, ANSYS CFX, a computational fluid dynamics (CFD) tool, has been used to conduct a numerical investigation. The research aims to investigate and analyze the pressure distribution on various surfaces of the building shape under the specified wind conditions^[13].

Sanyal, P. et al. (2022): The force, moment, and torsional coefficient predicting of a tall building with a triaxially symmetrical *Y* plan shape is the main objective of the work. The research begins with a Computational Fluid Dynamics (CFD) study using the RANS *k-ε* turbulence model. This research investigates the relationship between aerodynamic coefficient fluctuation and corner cut percentage and angle of attack (AOA), taking flow patterns into account and examining changes in coefficient values. Rational parametric equations for the aerodynamic coefficients are predicted using the CFD findings and design parameters. Additionally, Artificial Neural Networks (ANN) are trained using the results of CFD. The efficacy of the surrogate modeling is validated using wind tunnel data and compared to the outcomes of CFD, ANN, and rational parametric equations. Good predictability of the networks is indicated by the greatest observed error for ANN modeling, which is less than 4%^[14].

CHAPTER 3

METHODOLOGY

3.0 Modelling of isolated building

CFD simulation is done on two software platforms namely ANSYS Fluent and OpenFOAM.

Main components of the CFD are same i.e.

1. Computational Domain
2. Meshing
3. Boundary Conditions for inlet, outlets and walls.

3.1 Computational Domain

For the purpose of numerical simulation, the project assumes a prototype building of square plan with dimensions 10m x 10m in plan and 10m height. Based on the dimensions of the building the computational domain size for the numerical simulation is determined. The domain should be sufficiently large so as to prevent fluid streams from reflecting and creating unnatural pressure fields around the building model. From the study of literature, it can be found that from the obstruction present in the wind flow field, the lateral and top distance of the domain boundary should be at least $5H$ from obstruction, where H is the height of the obstruction (building). The distance of the obstruction from the inlet boundary should be adjusted to match the upwind area's appropriate roughness height. For the case under consideration $5H$ is taken as the distance of the obstruction (building) from the inlet boundary. For outflow boundary distance, it should be at least $10H$ from outer edge of the building (obstruction), this distance is taken as $15H$ for the case under consideration. All distances are measures from the respective outer edges of the building (*Fig. 6*) and all the boundary conditions used for the analysis in ANSYS is shown in *Fig. 7*. Modelling of prototype building in Open-Source software FreeCAD is presented in *Fig. 8*.

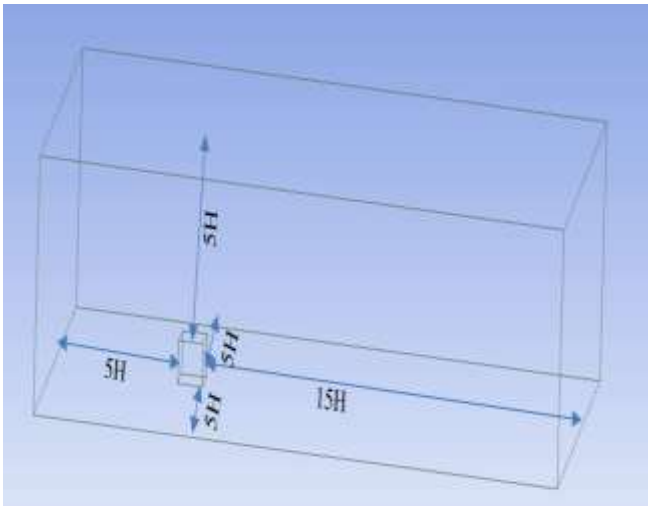


Figure 6 Prototype building with Wireframe Domain in ANSYS

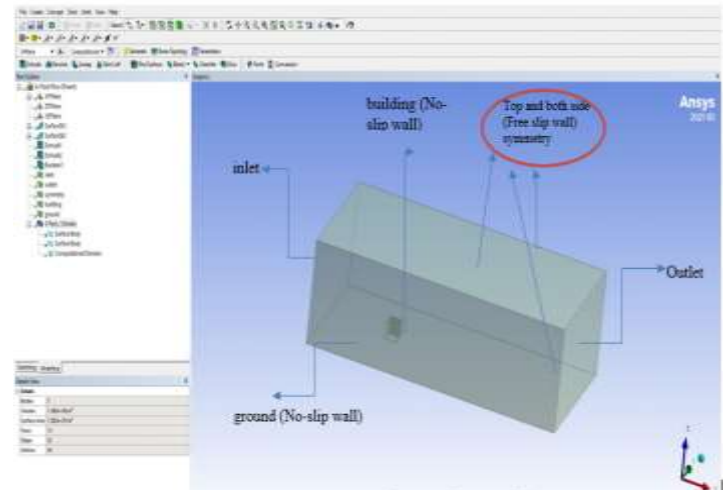


Figure 7 Model of prototype building in ANSYS design modular with boundary conditions



Figure 8 Prototype building with Computational Domain, Modelling in FreeCAD (Open Source)

3.2 Initial condition for both the software:

Inlet velocity = 10m/s (Constant)

Outlet pressure = 0 Pa

Top, both sides = symmetry (Free slip wall)

Ground = No slip wall

Building = No slip wall

3.3 Meshing:

3.3.1 ANSYS Meshing

Tetrahedral mesh (shown in Fig. 9) is provided with automatic method in ANSYS with refinement close to the building so as to accurately capture the wind velocity/pressure variation.

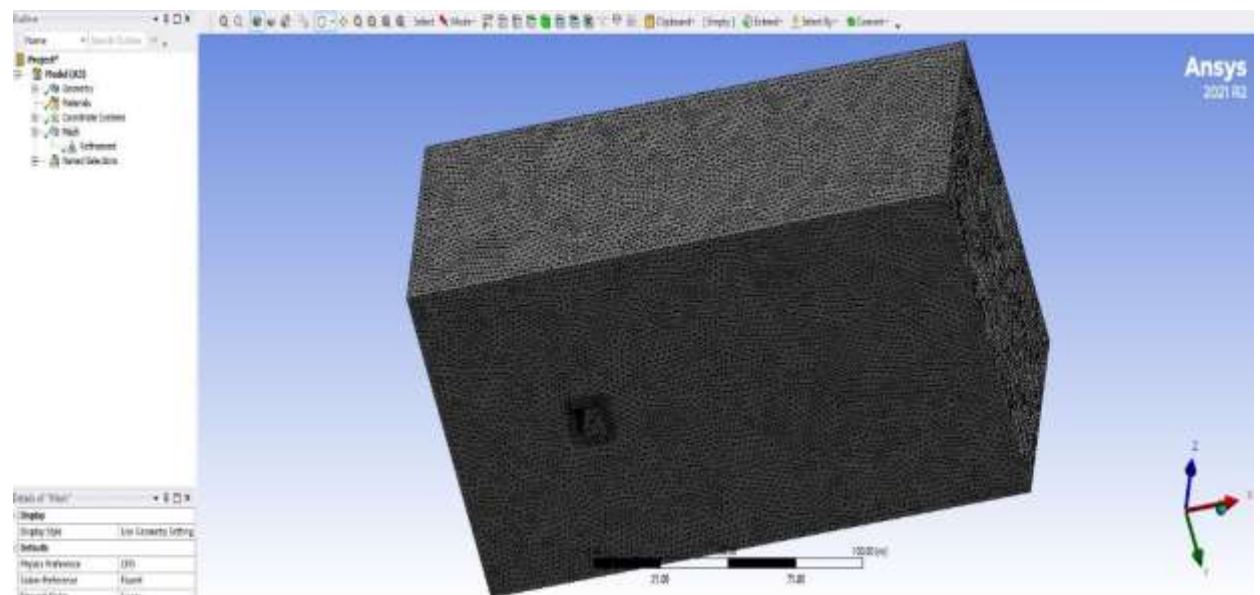


Figure 9 Meshing of Prototype building with refinement in ANSYS Fluent

Several meshing techniques were tried along with hexahedral meshing provided with inflation layers (shown in Fig. 10) close to the building, as well as polyhedral type using fluent solver and results were noted. For both the software platforms RANS steady analysis has been carried out. However, hexahedral

meshing (shown in *Fig.11*) provided with inflation layers close to the building was found to be the most efficient form for both the software platforms for the case under consideration.

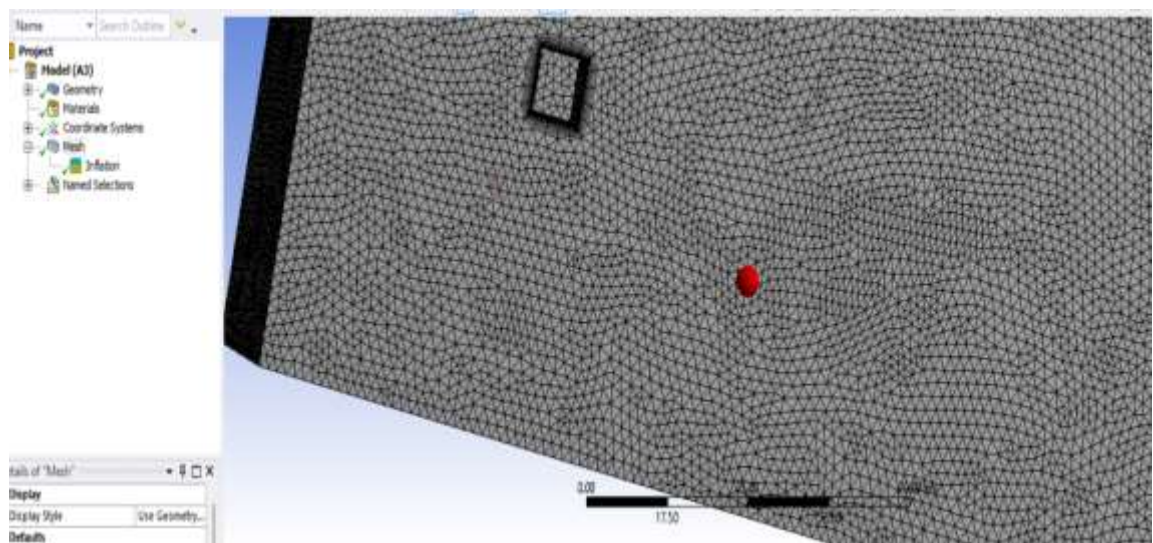


Figure 10 Tetrahedral Meshing with inflation (ANSYS)

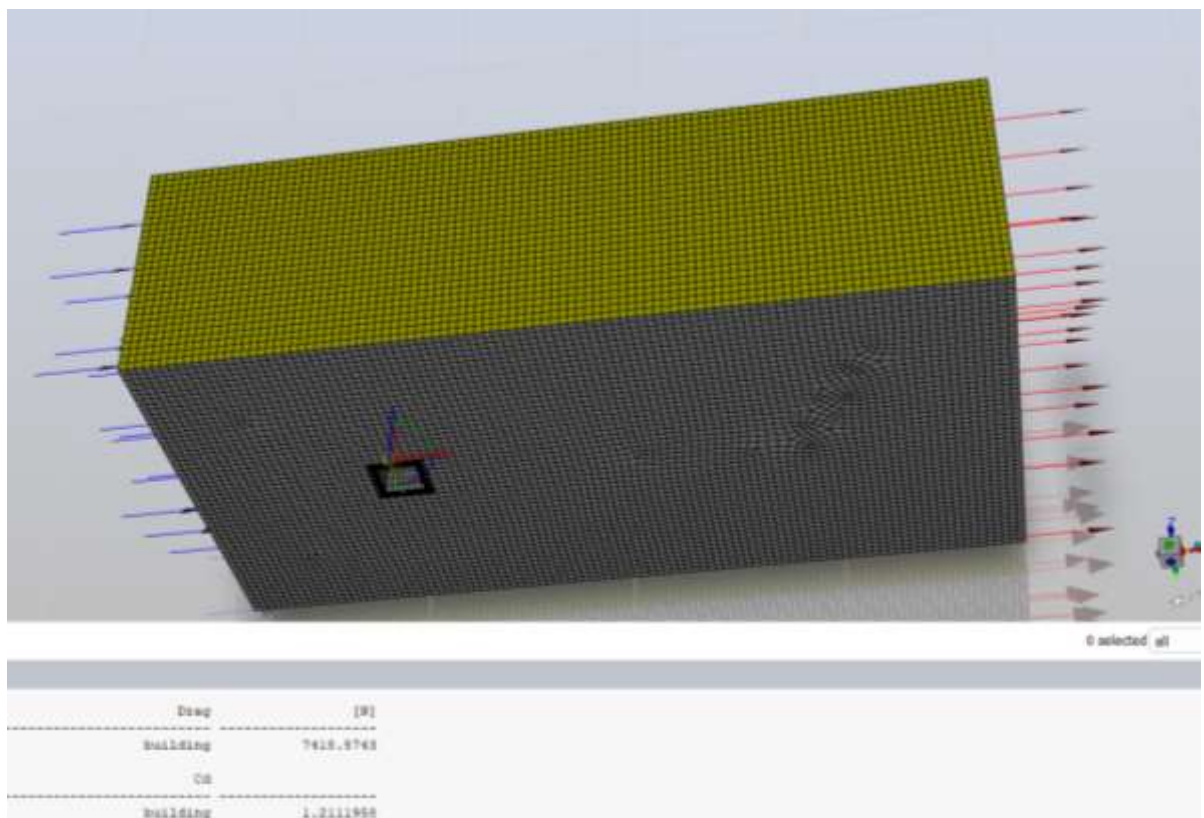


Figure 11 Hexahedral Meshing with Inflation (ANSYS)

3.3.2 OpenFOAM Meshing

In OpenFoam meshing can be created using command BlockMesh and Hexahedral meshing with refinement can be given using command snappyHexMesh.

There are also various Open-Source software that can be used for Modelling and Meshing namely Salome and FreeCAD etc. and Meshing can be Imported into OpenFoam by using different commands for different platform available in OpenFoam userguide i.e. ideasUnvToFoam for Salome and FluentMeshToFoam for ANSYS Fluent etc. Since our objective is to use Open-Source Software. Hence this project only uses Mesh of Open-Source software for OpenFoam. Salome Tetrahedral Mesh is presented in *Fig.12* and snappyHexMesh is presented in *Fig.13*.

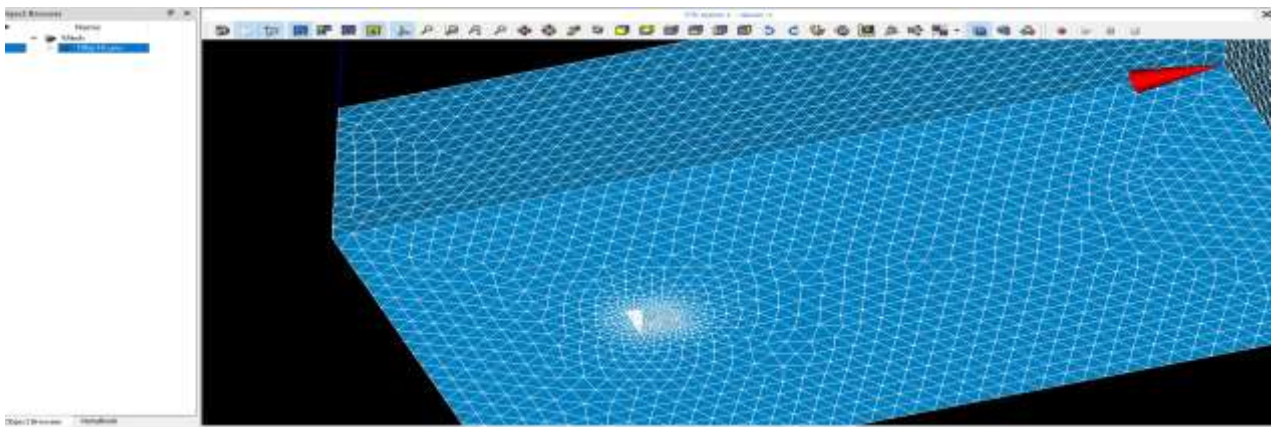


Figure 12 Tetrahedral Meshing (Salome open source)

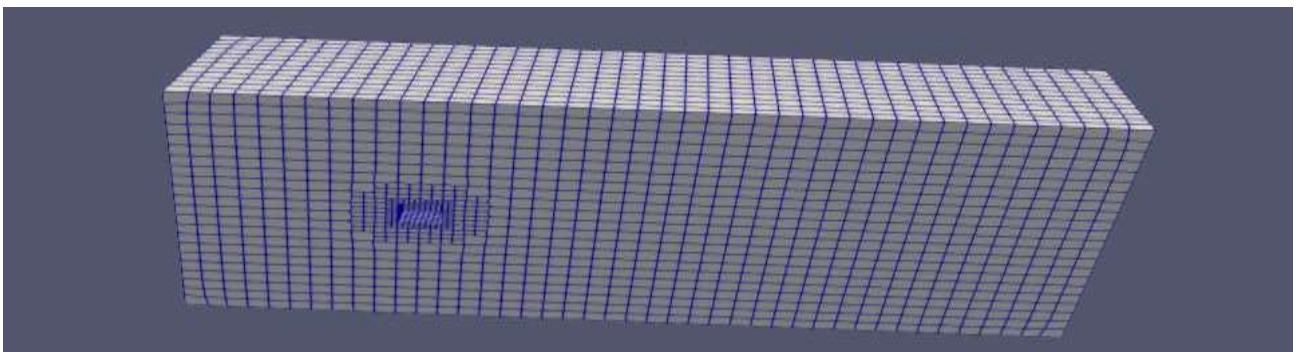


Figure 13 SnappyHexMesh/HexaHedral Mesh(OpenFoam)

CHAPTER 4

RESULTS AND DISCUSSION

All the calculation and analysis has been carried out for $k-\varepsilon$ turbulence viscous model in both software platforms i.e. ANSYS and OpenFoam and the results have been compared for constant inlet velocity of 10m/s.

4.1 Prototype building Analysis

4.1.1 For Tetrahedral meshing in ANSYS Fluent

Faces present in Prototype building are expressed in *Fig. 14*. Windward Face is A, Leeward face is B and side faces are Face C and D.

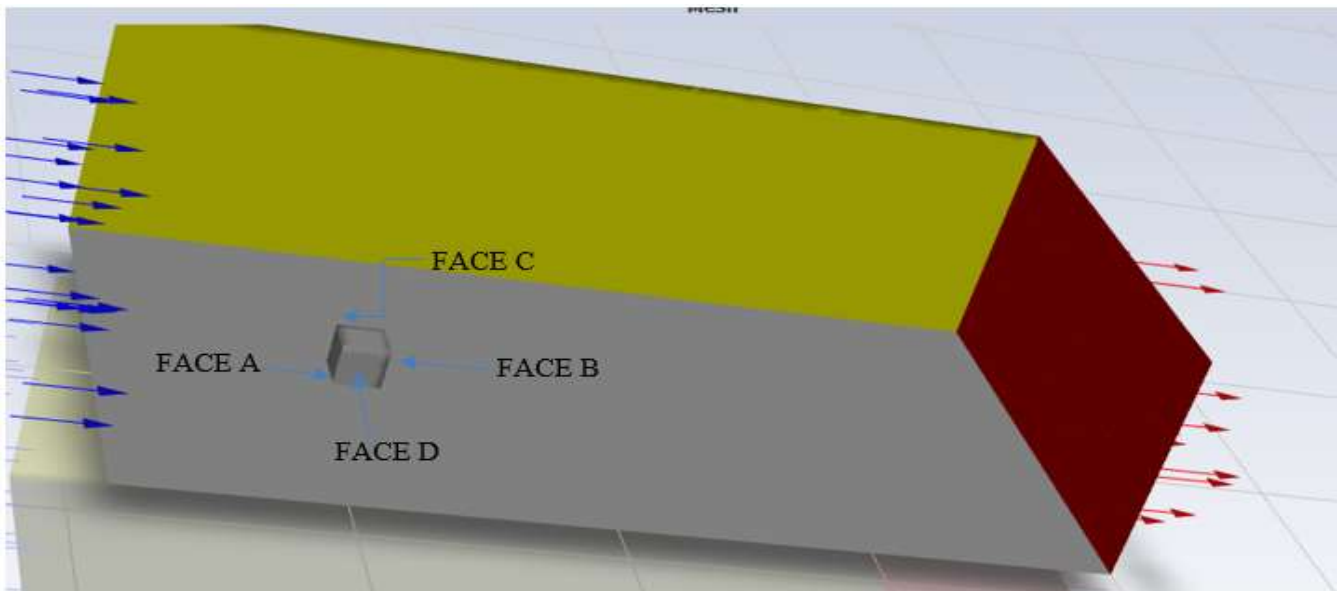
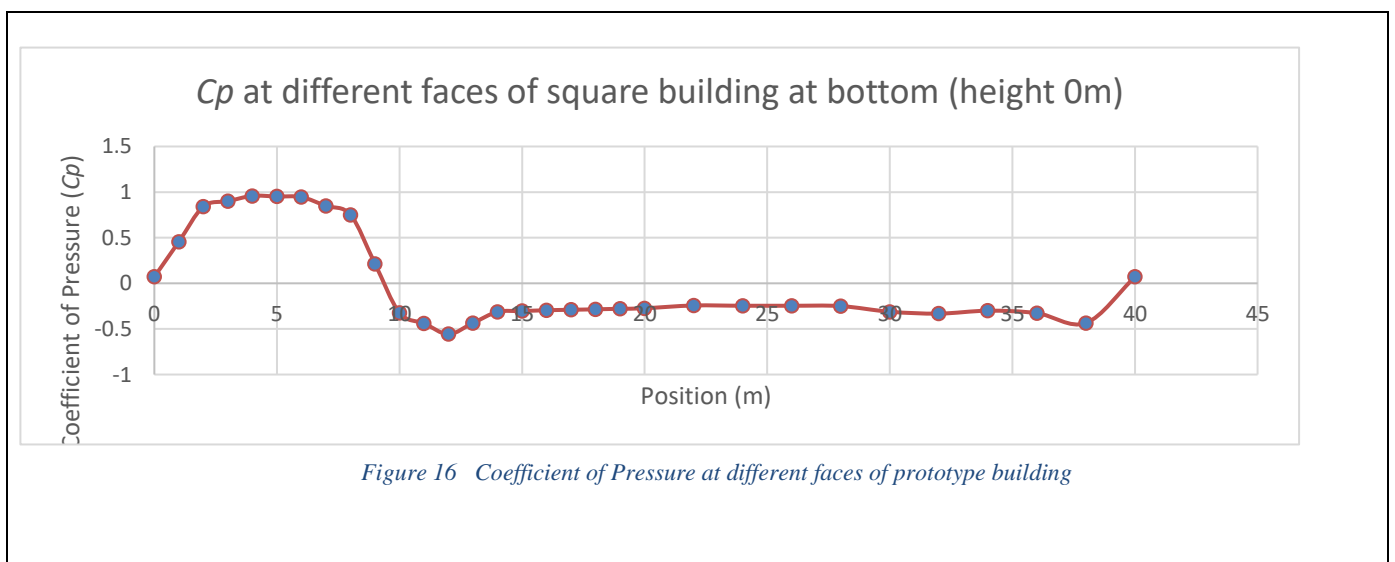
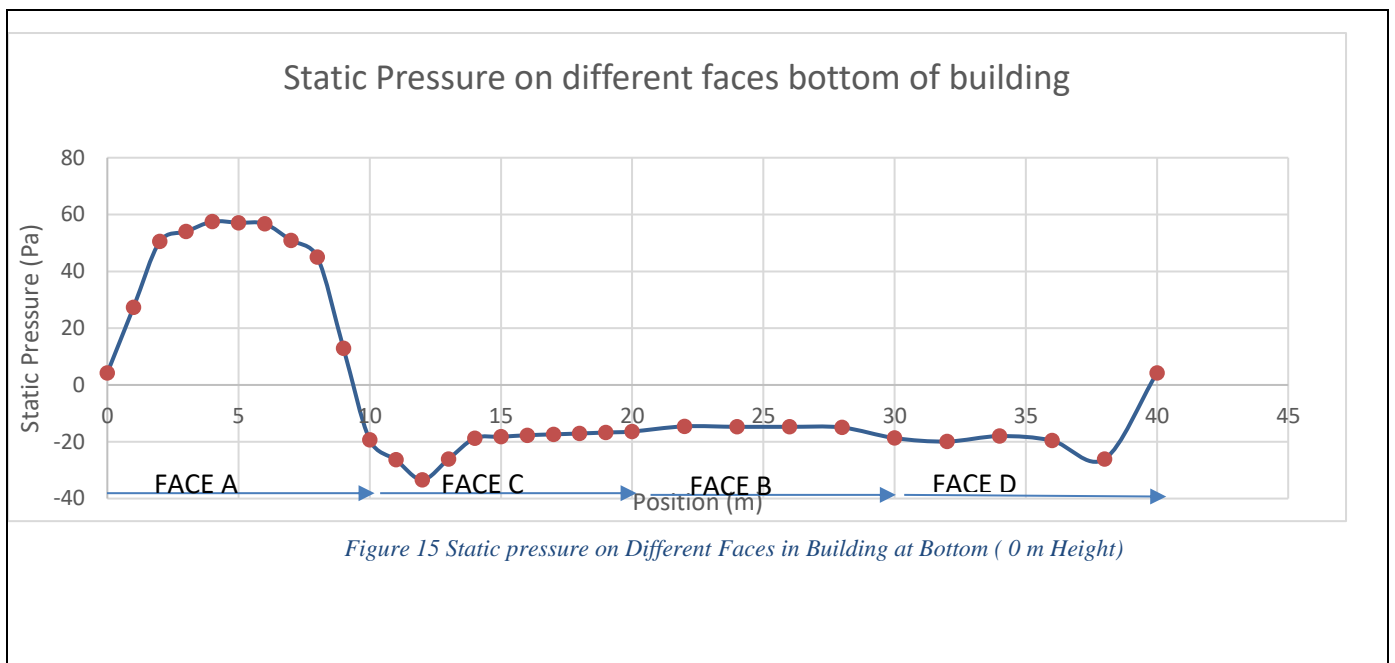


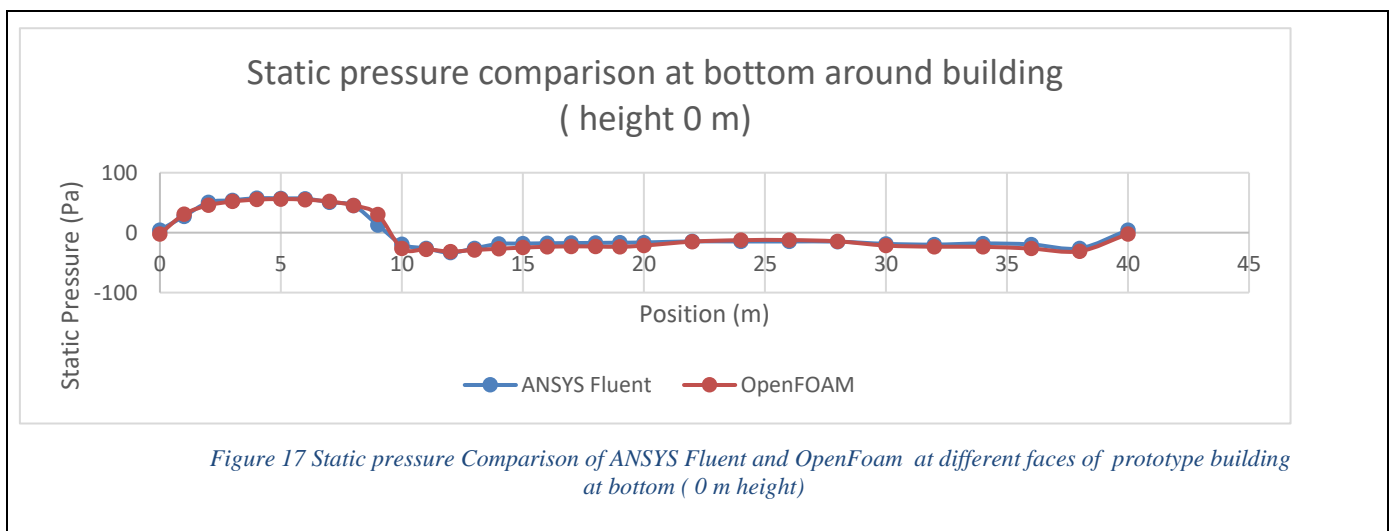
Figure 14 Face description of the prototype building

4.1.1.1 Analysis

Static wind pressure and wind coefficient of pressure is calculated at different part of building. Static wind pressure and Wind coefficient of pressure finding at bottom (0 m) height in ANSYS Fluent for tetrahedral meshing is presented in *Fig. 15* and *Fig. 16* respectively.



Wind Static pressure and Wind coefficient of pressure comparison at 0 m height are presented in *Fig. 17* and *Fig. 18* respectively.



Comparison of C_p in ANSYS Fluent and OpenFoam for prototype building at ground (0 m)

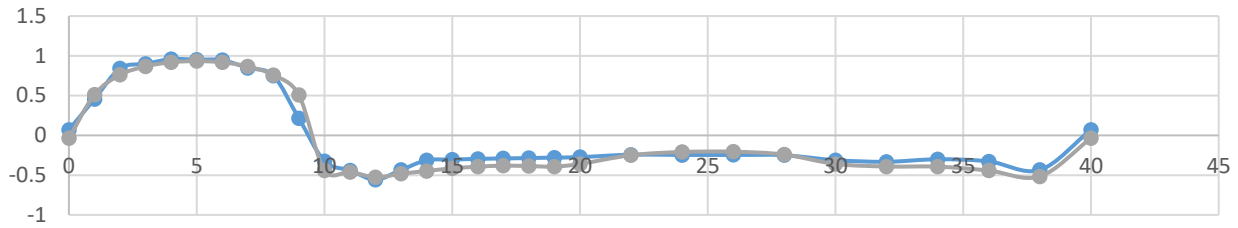


Figure 18 C_p Comparison of ANSYS Fluent and OpenFoam at bottom (0 m height)

4.1.1.2 Comparison of ANSYS Fluent and OpenFoam results with the help of graph

Wind Static pressure and Wind coefficient of pressure comparison at 5m height are presented in Fig. 19 and Fig. 20 respectively. Static wind pressure comparison at Vertical center-line at windward face is shown in Fig. 21.

Static pressure around building at mid height (5 m from ground)

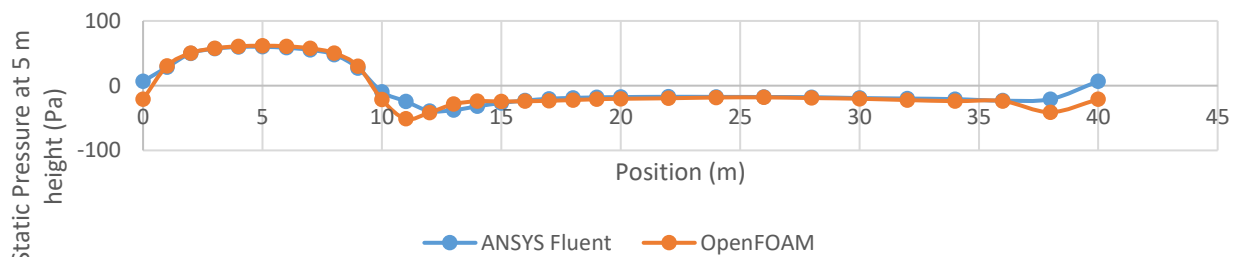


Figure 19 Static pressure Comparison of ANSYS Fluent and OpenFoam at different faces of prototype building at mid height (5 m height)

C_p Comparison at 5 m height / mid height of building

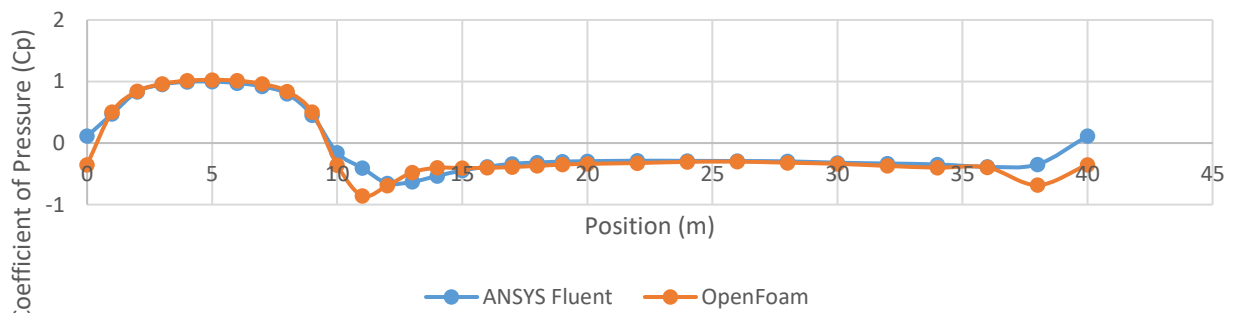


Figure 20 C_p Comparison of ANSYS Fluent and OpenFoam at mid height (5 m height)

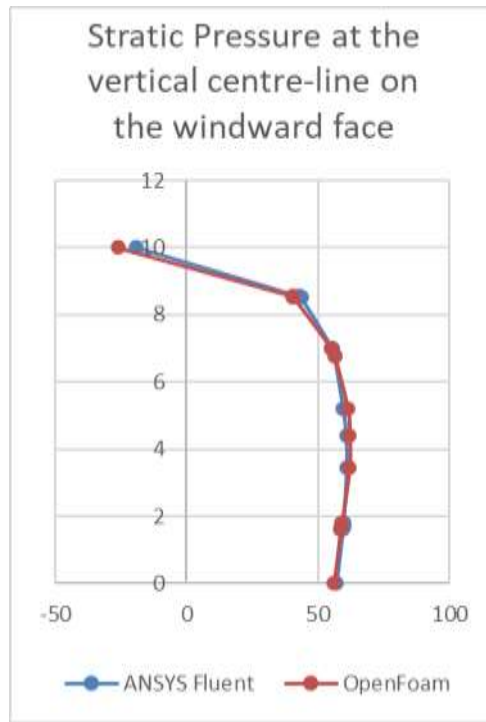


Figure 21 Static pressure magnitude at vertical line at 5m distance/ Centre-line

4.1.2 Visualization of results for Prototype building in ANSYS CFD Post

ANSYS Fluent uses their own ANSYS CFD Post tool for post processing and visualization of results. 2D plane can be inserted to get desired results. In *Fig. 22* A ZX plane is inserted to get the Velocity Streamline tracer shown in *Fig. 23*. Pressure contour can be seen in *Fig. 24* on obstacle building surfaces pn ANSYS CFD Post.

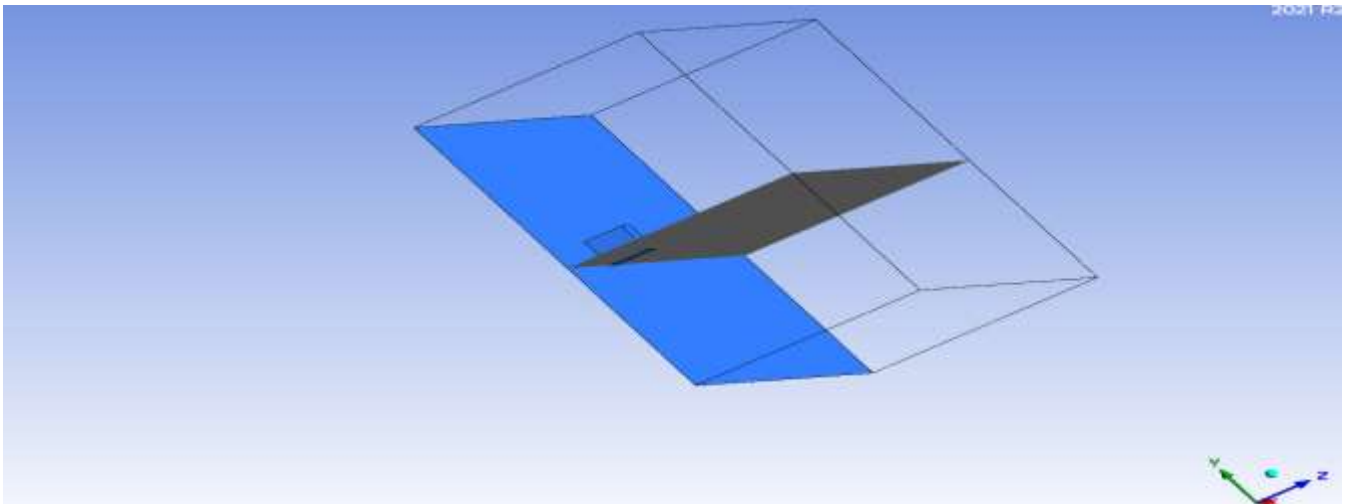


Figure 22 Wireframe diagram of square plan building with XZ plane just at the surface of D face

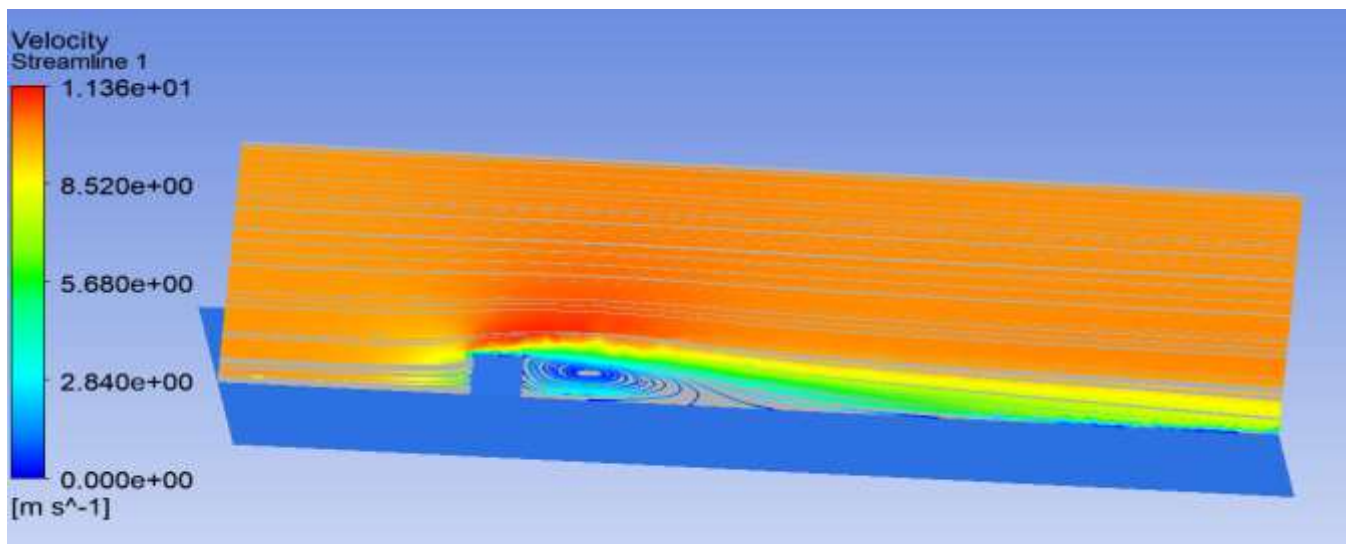


Figure 23 Velocity streamline at surface of D Face

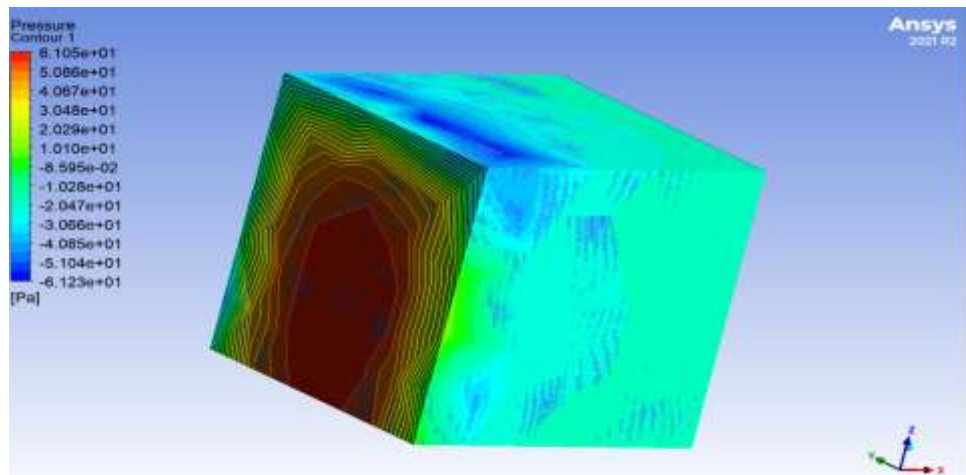


Figure 24 Pressure Contour of prototype building

4.1.3 Visualization of results for OpenFoam results of prototype building in paraview software (Free/Open Source)

OpenFoam don't have their own Post-processing tool/software but it uses the Freely available Open-Source post processing tool paraview. Post-processing of paraview is shown in Fig. 24, 25 ,26 and 27.

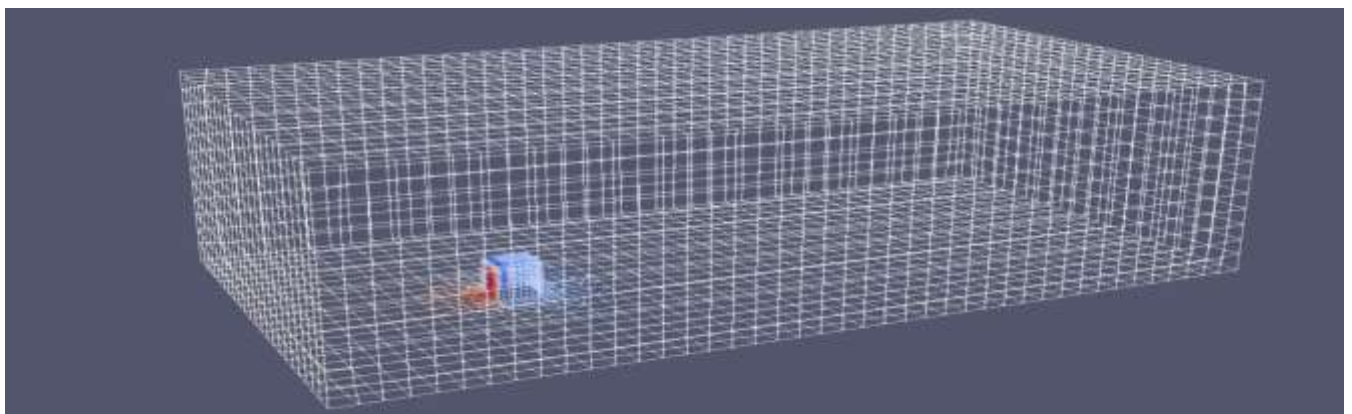


Figure 25 Wireframe diagram of prototype building in paraview

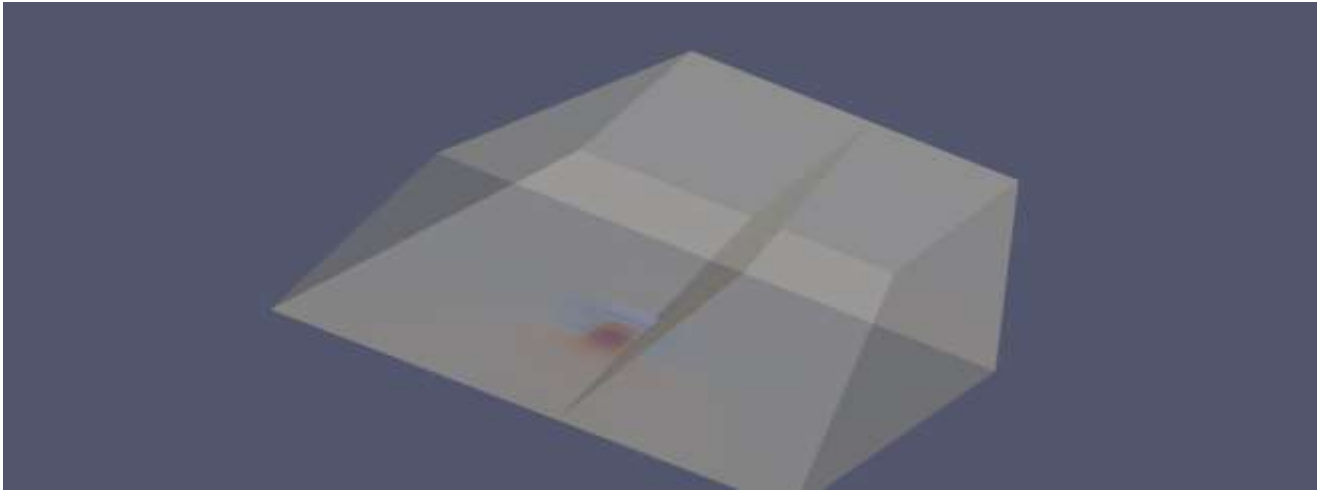


Figure 26 Plane at Face D in paraview

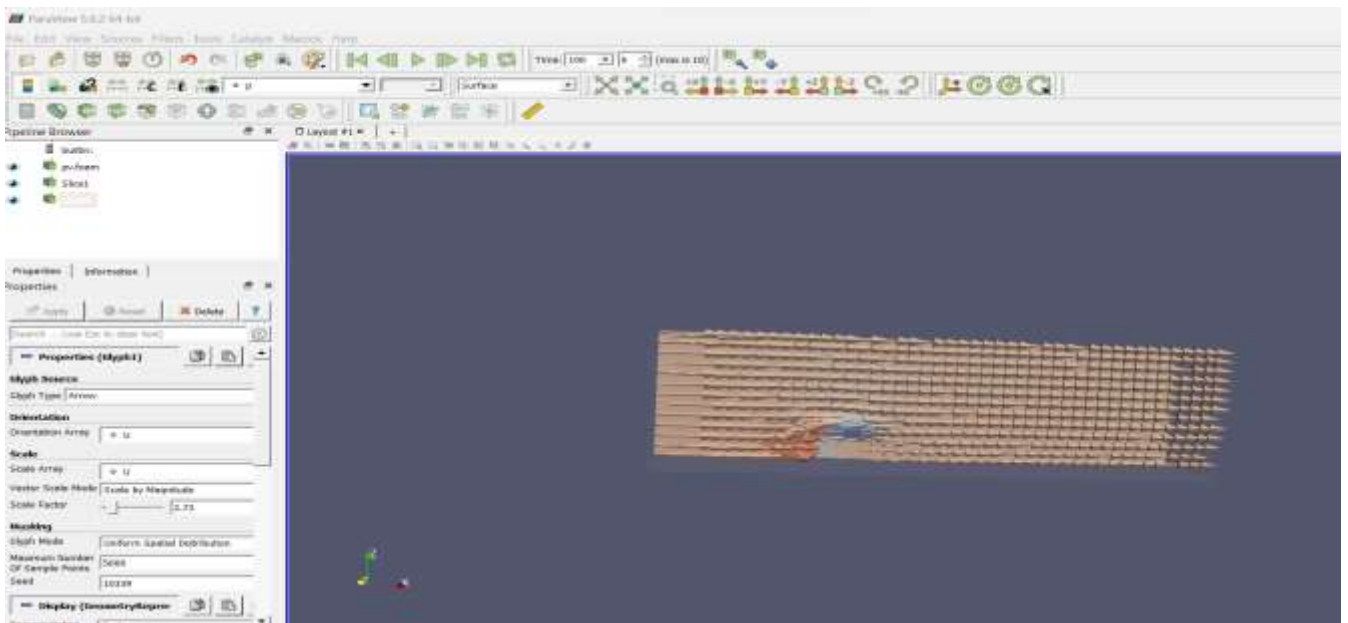


Figure 27 streamline tracer (paraview)

4.1.4 Drag Force and Drag Coefficient calculation diagram showing steps involved in paraview

OpenFoam don't have their any command for direct getting the value of Drag Force but Drag coefficient (C_d) can be get directly by editing of controlDict Directory inserting Force function with all reference values. From drag coefficient Drag Force can be calculated by

$$F_D = C_d \times \rho \frac{1}{2} AV^2$$

But In a Paraview software Drag Force can be calculated directly by extraction of block, surface and surface Normal. Paraview has their own calculator. F_D can be calculated using above Formula.

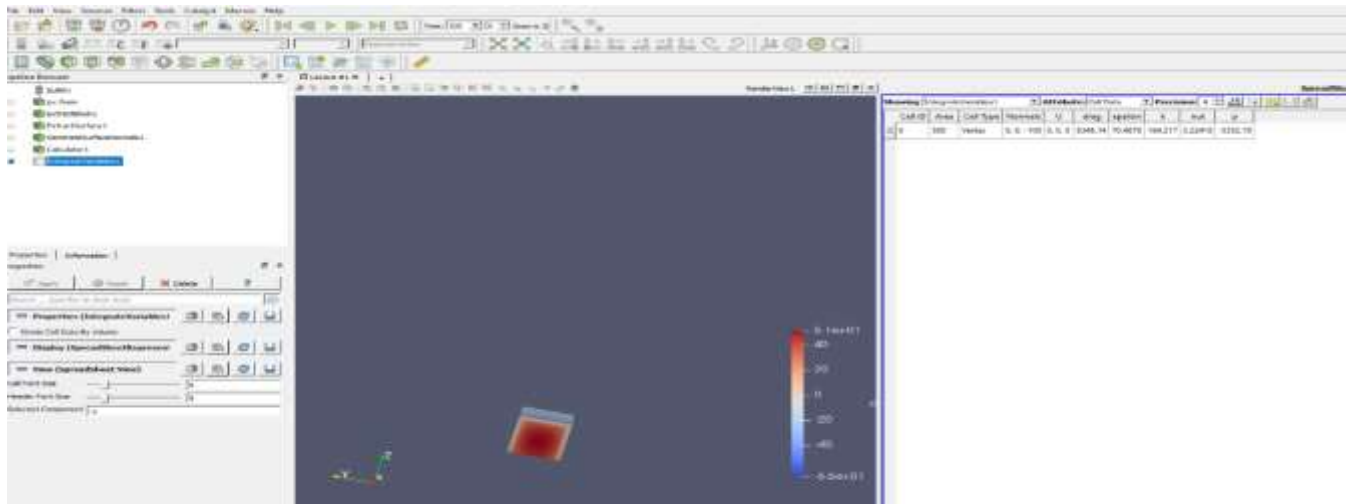


Figure 28 Drag Force calculation diagram showing steps involve in paraview

From the above calculation the Drag Force is **7329.86 N** in OpenFoam $k-\epsilon$ solution for prototype building and Drag coefficient is **1.196**.

4.1.5 Drag Force and Drag Coefficient calculation diagram showing steps involved in ANSYS Fluent Solver

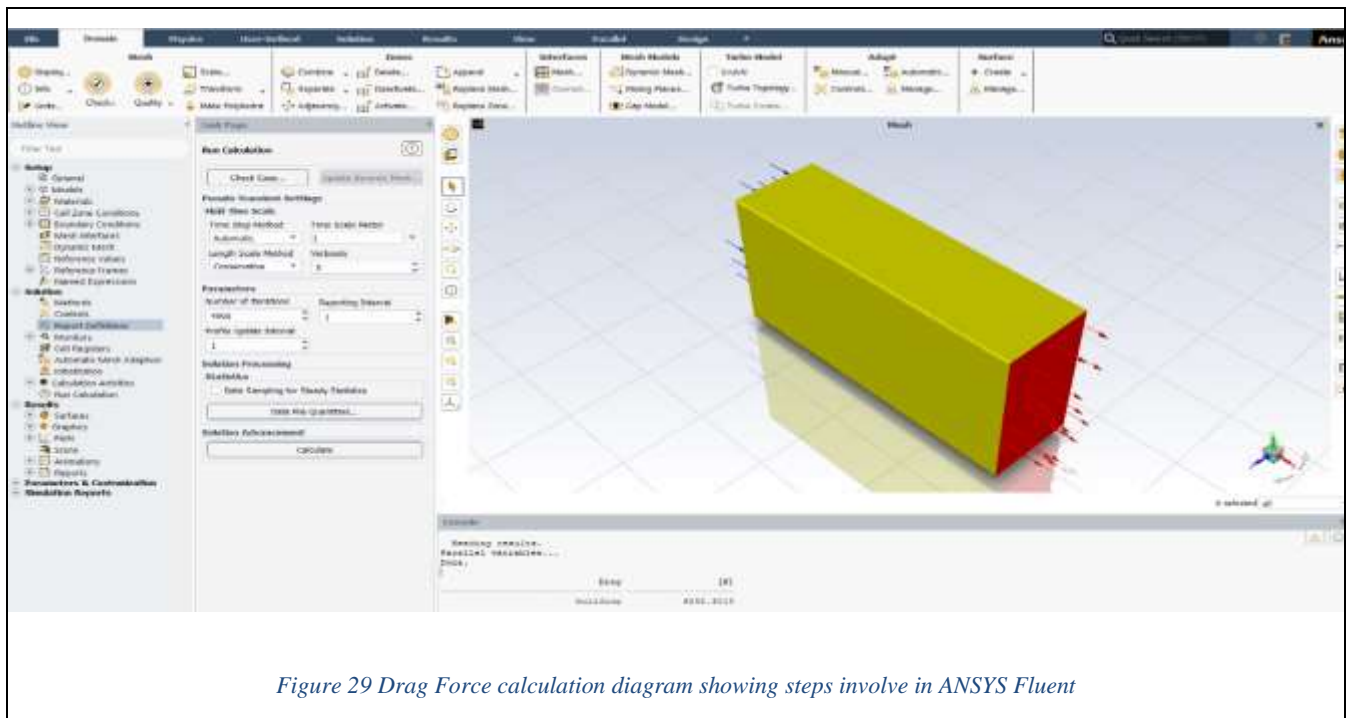


Figure 29 Drag Force calculation diagram showing steps involve in ANSYS Fluent

In ANSYS Fluent there is a simple command to calculate the Drag Force and Drag coefficient by inserting a reference values. However, Drag force is calculated by below Formula

Drag Force (F_D)= Static pressure (p) \times Surface Normal

And Drag Coefficient $C_d = \frac{F_D}{\frac{1}{2} \rho V^2 A}$

From the above calculation, Drag Force is **7418.5743 N** in Fluent k-epsilon solution for prototype building and Drag coefficient is **1.2111**.

4.1.6 Calculation of Static wind pressure and wind Coefficient of pressure C_p in different Faces by (Pressure average area Method)

FACE A (WINDWARD) OpenFoam					
Position (m)	Pressure (Pa)	Y coordinate	X Coordinate	Area	Pressure*Area
0.1	34.8843	0.3	10	3	104.6529
0.5	35.22	0.45	10	4.5	158.49
1	35.6572	0.5	10	5	178.286
1.5	36.2032	0.5	10	5	181.016
2	36.7509	0.5	10	5	183.7545
2.5	37.2308	0.5	10	5	186.154
3	37.3493	0.5	10	5	186.7465
3.5	37.469	0.5	10	5	187.345
4	37.2964	0.5	10	5	186.482
4.5	36.9191	0.5	10	5	184.5955
5	36.5362	0.5	10	5	182.681
5.5	35.8013	0.5	10	5	179.0065
6	35.0666	0.5	10	5	175.333
6.5	33.9611	0.5	10	5	169.8055
7	32.41029	0.5	10	5	162.0515
7.5	30.8619	0.5	10	5	154.3095
8	27.44767	0.5	10	5	137.2384
8.5	23.8625	0.5	10	5	119.3125
9	13.3218	0.5	10	5	66.609
9.5	-4.3302	0.45	10	4.5	-19.4859
9.9	-18.3688	0.3	10	3	-55.1064
					3009.277
					3686.364
				Average Static Pressure	36.86364
				C_p	0.614394

Table 2 C_p calculation for FACE A (OpenFoam)

FACE A (WINDWARD) ANSYS							
Position (m)	Static Pressure (Pa)		Y coordinate	X Coordinates	Area	Pressure * Area	
0.1	41.7641		0.3	10	3	125.2923	
0.5	41.9518		0.45	10	4.5	188.7831	
1	42.1864		0.5	10	5	210.932	
1.5	42.4209		0.5	10	5	212.1045	
2	42.6563		0.5	10	5	213.2815	
2.5	42.9525		0.5	10	5	214.7625	
3	43.2486		0.5	10	5	216.243	
3.5	43.5447		0.5	10	5	217.7235	
4	43.831		0.5	10	5	219.155	
4.5	43.3252		0.5	10	5	216.626	
5	42.8309		0.5	10	5	214.1545	
5.5	42.3365		0.5	10	5	211.6825	
6	41.8854		0.5	10	5	209.427	
6.5	42.4548		0.5	10	5	212.274	
7	43.0241		0.5	10	5	215.1205	
7.5	43.5934		0.5	10	5	217.967	
8	43.4004		0.5	10	5	217.002	
8.5	29.9746		0.5	10	5	149.873	
9	16.5487		0.5	10	5	82.7435	
9.5	3.1229		0.45	10	4.5	14.05305	
9.9	-7.6177		0.3	10	3	-22.8531	
	36.63979					3756.347	<i>Cp</i>
	0.610663					37.56347	0.626058

Table 3 *Cp* at Face A ANSYS

OpenFoam FACE B							
Position (m)	Pressure (Pa)		Y Coordinate	X coordinate	Area	Pressure*Area	
0.1	-12.0539		0.3	10	3	-36.1617	
0.5	-11.8444		0.45	10	4.5	-53.2998	
1	-11.582		0.5	10	5	-57.91	
1.5	-11.4774		0.5	10	5	-57.387	
2	-11.466		0.5	10	5	-57.33	
2.5	-11.5657		0.5	10	5	-57.8285	
3	-12.2221		0.5	10	5	-61.1105	
3.5	-12.8791		0.5	10	5	-64.3955	
4	-13.6955		0.5	10	5	-68.4775	
4.5	-14.6267		0.5	10	5	-73.1335	
5	-15.5554		0.5	10	5	-77.777	
5.5	-16.2468		0.5	10	5	-81.234	
6	-16.938		0.5	10	5	-84.69	
6.5	-17.3741		0.5	10	5	-86.8705	
7	-17.5091		0.5	10	5	-87.5455	
7.5	-17.6433		0.5	10	5	-88.2165	
8	-17.2802		0.5	10	5	-86.401	
8.5	-16.8684		0.5	10	5	-84.342	
9	-16.5622		0.5	10	5	-82.811	

9.5	-16.347		0.45	10	4.5	-73.5615	
9.9	-16.1765		0.3	10	3	-48.5295	
						-1469.01	Cp
						-1799.54	-0.36741

Table 4 Cp at Face B in OpenFoam

OpenFoam FACE C/D							
Position (m)	Pressure (Pa)		Y Coordinate	X coordinate	Area	Pressure*Area	
0.1	-20.1204		0.3	10	3	-60.3612	
0.5	-20.3509		0.45	10	4.5	-91.5791	
1	-20.6373		0.5	10	5	-103.187	
1.5	-20.9747		0.5	10	5	-104.874	
2	-21.3853		0.5	10	5	-106.927	
2.5	-21.7762		0.5	10	5	-108.881	
3	-22.0701		0.5	10	5	-110.351	
3.5	-22.3629		0.5	10	5	-111.815	
4	-22.5906		0.5	10	5	-112.953	
4.5	-22.7647		0.5	10	5	-113.824	
5	-22.9377		0.5	10	5	-114.689	
5.5	-22.8843		0.5	10	5	-114.422	
6	-22.83		0.5	10	5	-114.15	
6.5	-22.6807		0.5	10	5	-113.404	
7	-22.4229		0.5	10	5	-112.115	
7.5	-22.1649		0.5	10	5	-110.825	
8	-21.6796		0.5	10	5	-108.398	
8.5	-21.1808		0.5	10	5	-105.904	
9	-21.3659		0.5	10	5	-106.83	
9.5	-22.1686		0.45	10	4.5	-99.7587	
9.9	-22.8155		0.3	10	3	-68.4465	
						-2193.69	Cp
						-2687.27	-0.54865

Table 5 Cp at Face C/D in OpenFoam

ANSYS FACE C/D							
Position (m)	Pressure (Pa)		Y Coordinate	X coordinate	Area	Pressure*Area	
0.1	-24.4171		0.3	10	3	-73.2514	
0.5	-24.5102		0.45	10	4.5	-110.296	
1	-24.6266		0.5	10	5	-123.133	
1.5	-24.743		0.5	10	5	-123.715	
2	-24.858		0.5	10	5	-124.29	
2.5	-24.8762		0.5	10	5	-124.381	
3	-24.8943		0.5	10	5	-124.472	
3.5	-24.9125		0.5	10	5	-124.562	
4	-24.9335		0.5	10	5	-124.667	
4.5	-25.0573		0.5	10	5	-125.287	

5	-25.1812		0.5	10	5	-125.906	
5.5	-25.3051		0.5	10	5	-126.525	
6	-25.4103		0.5	10	5	-127.052	
6.5	-25.0795		0.5	10	5	-125.398	
7	-24.7487		0.5	10	5	-123.743	
7.5	-24.4178		0.5	10	5	-122.089	
8	-24.1403		0.5	10	5	-120.701	
8.5	-24.786		0.5	10	5	-123.93	
9	-25.4317		0.5	10	5	-127.159	
9.5	-26.0774		0.45	10	4.5	-117.348	
9.9	-26.5941		0.3	10	3	-79.7822	
						-2497.69	Cp
						-24.9769	-0.41628

Table 6 Cp at FACE C/D ANSYS

ANSYS FACE B							
Position (m)	Pressure (Pa)		Y Coordinate	X coordinate	Area	Pressure*Area	
0.1	-16.211		0.3	10	3	-48.633	
0.5	-16.2624		0.45	10	4.5	-73.1808	
1	-17.0021		0.5	10	5	-85.0105	
1.5	-16.3908		0.5	10	5	-81.954	
2	-16.4577		0.5	10	5	-82.2885	
2.5	-16.7162		0.5	10	5	-83.581	
3	-16.9746		0.5	10	5	-84.873	
3.5	-17.2331		0.5	10	5	-86.1656	
4	-17.4962		0.5	10	5	-87.4811	
4.5	-17.9241		0.5	10	5	-89.6204	
5	-18.3519		0.5	10	5	-91.7597	
5.5	-18.7798		0.5	10	5	-93.899	
6	-19.1977		0.5	10	5	-95.9884	
6.5	-19.3822		0.5	10	5	-96.9109	
7	-19.5667		0.5	10	5	-97.8333	
7.5	-19.7512		0.5	10	5	-98.7558	
8	-19.9544		0.5	10	5	-99.7721	
8.5	-20.4821		0.5	10	5	-102.411	
9	-21.0098		0.5	10	5	-105.049	
9.5	-21.5375		0.45	10	4.5	-96.9185	
9.9	-21.9596		0.3	10	3	-65.8788	
						-1847.96	Cp
						-18.4796	-0.30799

Table 7 Cp at FACE B in ANSYS

Coefficient of pressure (C_p) for different faces has been calculated by pressure-average area method and got the following results:

FACE	Value of C_p as per ANSYS Fluent	Value of C_p as per OpenFoam	Value of C_p as per IS:875 (part-3)
FACE A	0.626058	0.614394	0.7
FACE B	-0.30799	-0.36741	0.25
FACE C AND D	-0.41628	-0.54865	0.6

Table 8 Summarised Value of C_p in different faces

From the IS:875 (Part 3):2015 as per clause 7.3.3.1 Value of C_p for different Faces

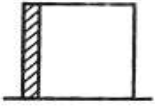
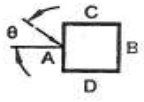
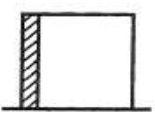
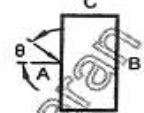
$\frac{1}{2} < \frac{h}{w} \leq \frac{3}{2}$	$1 \leq \frac{l}{w} \leq \frac{3}{2}$			0 90	+0.7 -0.6	-0.25 -0.6	-0.6 +0.7	-0.6 -0.25	} -1.1
	$\frac{3}{2} \leq \frac{l}{w} < 4$			0 90	+0.7 -0.5	-0.3 -0.5	-0.7 +0.7	-0.7 -0.1	

Figure 30 Value of C_p for different Faces as per Clause 7.3.3.1

From the IS875(part 3):2015 as per Fig. 4/ Clause 7.4.2, Value of Drag coefficient

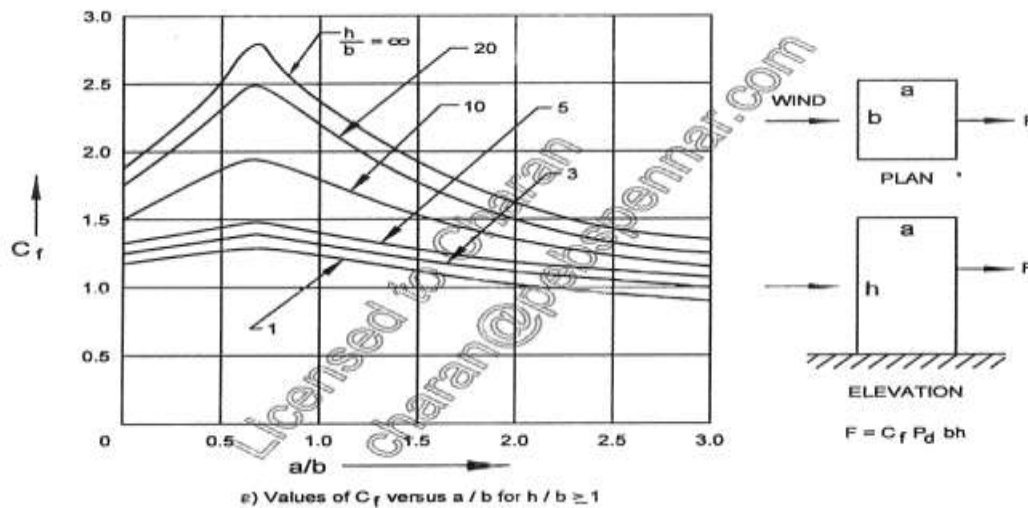


Figure 31 Value of Drag Coefficient for building as per clause 7.4.2

From the Graph of IS:875 (part 3) clause 7.4.2 Value of Drag coefficient is found approximately 1.26.

CHAPTER 5 CONCLUSIONS

From the above obtained results it has been observed that the two software platforms compete with each other in a very close manner and have dominance over one and another for different faces of the building. Drag Coefficient (Drag Force) value obtained in ANSYS is noted to be more accurate while Coefficient of pressure (C_p) values obtained in OpenFoam are more precise. Error is less than 20% (in force and pressure) for both software platforms. Both the software platforms gave approximately same pressure values at different locations of the building. Velocity streamline are following the same path in both the software platforms. All the post processing and result visualization has been done in paraview for OpenFoam while ANSYS has their own post processing tool called CFD post. Major derived conclusions from the obtained results are:

1. From OpenFoam platform, Drag Force is **7329.86 N** and Drag Coefficient is **1.196** for k- ϵ turbulence model. Indian standard Code IS:875(part-3) has Drag coefficient 1.26. Error is 5.079% which is below 20%.
2. From ANSYS Fluent platform, Drag Force is **7418.5743 N** and Drag Coefficient is **1.2111** for k- ϵ turbulence model for prototype. Code IS:875(part-3) has Drag coefficient 1.26. Error is 3.88% which is below 20%.
3. As per code IS:875(part-3), The sum of C_p for windward and leeward face should be $0.7+(0.25)=0.95$. OpenFoam gives sum $0.61+(0.36)=0.97$, which has 2.105% error. ANSYS Fluent gives $0.6260+(0.30799)=0.93$, which again has 2.105% error.
4. Maximum/Positive pressure is 47.023Pa in OpenFoam and 43.831Pa in ANSYS which is lies between 3.5m to 4m height of building at windward face/Face A on both the software platforms.
5. Lowest/Maximum suction pressure is -28.089Pa in OpenFoam and -25.41Pa in ANSYS which is lies between 5m to 6m height of building found on side Face C/D on both the software platforms.

REFERENCES

- [1]. Weerasuriya, A. U. (2013, July 30). Computational Fluid Dynamic (CFD) simulation of flow around tall buildings. *Engineer: Journal of the Institution of Engineers, Sri Lanka*, 46(3), 43. <https://doi.org/10.4038/engineer.v46i3.6784>.
- [2]. ANSYS, ANSYS Fluent User Guide 13.0 ANSYS, Inc.
- [3]. OpenFOAM: User Guide V2112.
- [4]. Blocken, B. B., Stathopoulos, T., & Van Beeck, J. P. a. J. (2016). Pedestrian-level wind conditions around buildings: Review of wind-tunnel and CFD techniques and their accuracy for wind comfort assessment. *Building and Environment*, 100, 50–81. <https://doi.org/10.1016/j.buildenv.2016.02.004>.
- [5]. Calzolari, G., & Liu, W. (2021). Deep learning to replace, improve, or aid CFD analysis in built environment applications: A review. *Building and Environment*, 206, 108315. <https://doi.org/10.1016/j.buildenv.2021.108315>.
- [6]. Zaki, A., & Sharma, R. N. (2023). Wind-tunnel analysis of turbulent flow in cross-ventilated buildings with windcatchers: Impact of surrounding buildings. *Building and Environment*, 244, 110826. <https://doi.org/10.1016/j.buildenv.2023.110826>.
- [7]. Yuan, Y., Yan, B., Zhou, X., Yang, Q., Huang, G., He, Y., & Yan, J. (2022). RANS simulations of aerodynamic forces on a tall building under twisted winds considering horizontal homogeneity. *Journal of Building Engineering*, 54, 104628. <https://doi.org/10.1016/j.jobee.2022.104628>.
- [8]. Liu, J., Hui, Y., Yang, Q., & Zhang, R. (2023). LES evaluation of the aerodynamic characteristics of high-rise building with horizontal ribs under atmospheric boundary layer flow. *Journal of Building Engineering*, 71, 106487. <https://doi.org/10.1016/j.jobee.2023.106487>.
- [9]. Wijesooriya, K., Mohotti, D., Amin, A., & Chauhan, K. (2021). Wind loads on a super-tall slender structure: A validation of an uncoupled fluid-structure interaction (FSI) analysis. *Journal of Building Engineering*, 35, 102028. <https://doi.org/10.1016/j.jobee.2020.102028>.
- [10]. Chauhan, B. S., & Ahuja, A. K. (2020). RESPONSE OF TALL BUILDING SUBJECTED TO WIND LOADS UNDER INTERFERENCE CONDITION. *International Journal of Civil Engineering and Technology*, 11(2), 156-163. <https://doi.org/10.34218/ijciet.11.2.2020.015>.

[11]. Chauhan, B. S., Ahuja, A. K., & Chakrabarti, A. (2023). Study of Variation in Wind Loads on Rectangular Cross-section Tall Building due to Change in Location of Interfering Buildings. *Arabian Journal for Science and Engineering*, 48(10), 12825–12844. <https://doi.org/10.1007/s13369-022-07582-y>.

[12]. Chauhan, B. S., & Ahuja, A. K. (2017). Effect of height variation of closely located interfering buildings on wind loads on tall buildings. *International Journal of Earth Sciences and Engineering*, 10(02), 378–382. <https://doi.org/10.21276/ijee.2017.10.0235>.

[13]. Mukherjee, S., Chakraborty, S., Dalui, S. K., & Ahuja, A. K. (2014). Wind induced pressure on “Y” plan shape tall building. *Wind and Structures*, 19(5), 523–540. <https://doi.org/10.12989/was.2014.19.5.523>.

[14]. Sanyal, P., & Dalui, S. K. (2022). Forecasting of aerodynamic coefficients of tri-axially symmetrical Y plan shaped tall building based on CFD data trained ANN. *Journal of Building Engineering*, 47, 103889. <https://doi.org/10.1016/j.job.2021.103889>.